TECHNICAL REPORT STANDARD TITLE PAGE

1. REPORT NO.	2. GOVERNMENT ACCESSION NO.	3. RECIPIENT'S CATALOG NO.
WA-RD 447.1		

4. TITLE AND SUBTITLE	5. REPORT DATE
Fatigue Cracking of Riveted Steel Tied Arch and Truss Bridges	March 1998
	6. PERFORMING ORGANIZATION CODE
7. AUTHOR(S)	8. PERFORMING ORGANIZATION REPORT NO.
Charles W. Roeder, Gregory A. MacRae, Kyoko Arima, Paul N. Crocker, Scott D. Wong	
9. PERFORMING ORGANIZATION NAME AND ADDRESS	10. WORK UNIT NO.
Washington State Transportation Center (TRAC) University of Washington, Bx 354802 University District Building; 1107 NE 45th Street, Suite 535 Seattle, Washington 98105-4631	11. CONTRACT OR GRANT NO. Contract T9903, Task 60
12. SPONSORING AGENCY NAME AND ADDRESS	13. TYPE OF REPORT AND PERIOD COVERED
Washington State Department of Transportation Transportation Building, MS 7370 Olympia, Washington 98504-7370	Research Report
	14. SPONSORING AGENCY CODE

15. SUPPLEMENTARY NOTES

This study was conducted in cooperation with the U.S. Department of Transportation, Federal Highway Administration.

16. ABSTRACT

Riveted steel truss and tied arch bridges in Washington state have experienced significant cracking that is due to fatigue loading. The Lewis River and Toutle River bridges are good examples of these two bridge types. They are both on the southbound lanes of Interstate 5 and experience heavy truck traffic. This research study addressed the fatigue cracking on these two bridges.

The cracking on these two bridges was summarized and analyzed. Computer models of the two bridges were developed, and static and dynamic analyses of the bridges were performed. Instrumentation was installed on both bridges in 1996. Controlled load and weight station tests were performed on the two bridges with trucks of known weight and geometry traveling at known speeds. The results of these measurements were used to evaluate the overall behavior of the two bridges and to calibrate the instruments for further testing with trucks of unknown weight and geometry.

Upon completion of the calibration tests, uncontrolled truck traffic was measured for the two bridges over 3 to 4 weeks. Extensive data were obtained for the two bridges, and load spectra were developed. These were combined with historic truck traffic data and predictions for future traffic in the I-5 corridor, and fatigue was estimated for critical components of the two bridges.

The Toutle River bridge was found to be very sensitive to dynamic vibration under truck loading, and fatigue cracking noted in the floorbeams of this bridge was found to be deformation driven. There is also a potential for stress driven fatigue cracking in the tie chord in coming years.

The Lewis River bridge was found to have serious fatigue cracking potential in the copes of the stringers for the deck system. There is less serious potential for fatigue cracking at the cover plate terminations of the floorbeams. There appears to be little potential for fatigue cracking in the truss members, unless there is an extreme nonuniform distribution of stress through the built-up members.

The ramifications of the fatigue cracking and possible repairs and modifications were evaluated.

17. KEY WORDS	18. DISTRIBUTION STATEMENT
Bridge fatigue cracking, steel truss bridges, tied arch bridges	No restrictions. This document is available to the public through the National Technical Information Service, Springfield, VA 22616

19. SECURITY CLASSIF. (of this report)	20. SECURITY CLASSIF. (of this page)	21. NO. OF PAGES	22. PRICE
None	None	89	

Research Report
Research Project T9903, Task 60
Steel Bridge Cracking

FATIGUE CRACKING OF RIVETED STEEL TIED ARCH AND TRUSS BRIDGES

by

Charles W. Roeder
Gregory A. MacRae
Paul N. Crocker
Kyoko Arima
Scott D. Wong

Department of Civil Engineering
University of Washington, Bx 352700
Seattle, Washington 98195-2700

Washington State Transportation Center (TRAC)
University of Washington, Box 354802
University District Building
1107 NE 45th Street, Suite 535
Seattle, Washington 98105-4631

Washington State Department of Transportation
Technical Monitor
Edward Henley, Bridge Management Engineer
Bridge and Structures

Prepared for

Washington State Transportation Commission
Department of Transportation
and in cooperation with
U.S. Department of Transportation
Federal Highway Administration

March 1998

DISCLAIMER

The contents of this report reflect the views of the authors, who are responsible for the facts and the accuracy of the data presented herein. The contents do not necessarily reflect the official views or policies of the Washington State Transportation Commission, Department of Transportation, or the Federal Highway Administration. This report does not constitute a standard, specification, or regulation.

TABLE OF CONTENTS

EXECUTIVE SUMMARY ix

INTRODUCTION 1

Research Objective 1
The Problem 1
Specific Issues 6

REVIEW OF PREVIOUS WORK 11

Literature Review 11
Correlation of Existing Knowledge to Riveted Bridges 19

BRIDGE MODELING AND INSTRUMENTATION 21

Bridge Modeling and Predicted Global Behavior 21
Predicted Local Behavior 23
Instrumentation 25

CONTROLLED TESTS ON BRIDGES 32

WSDOT Truck Testing 33
Free Vibration Response 37
Forced Vibration Tests 39
End Restraint and Composite Action of Floorbeams 41
End Restraint and Composite Action of Stringers 44
Bridge Deflections During Controlled Testing 49
Weigh Station Testing 50

UNCONTROLLED TRAFFIC MEASUREMENTS AND FATIGUE LIFE 54

General Comments 54
Uncontrolled Field Measurements 54
Frequency and Load Spectrum 56
Fatigue Life Estimates 62
Stringer Cope at Stringer to Floorbeam Connection 63
Floorbeams and Floorbeam to Chord Connections 66
Fatigue of Truss Members 69
Chord and Arch Members 71
Distortional Fatigue 72

SUMMARY, CONCLUSIONS AND RECOMMENDATIONS 77

Summary 77
Conclusions 77
Discussion of Recommendations 82

REFERENCES 88

LIST OF FIGURES

Figure		Page
1.	Typical Layout of Structural Systems for the Deck of Steel Truss and Tied Arch Bridges	2
2.	Typical Stringer to Floor Beam Connections; a) Coped Web Angle Connections, b) Stiffened Seat Connections	3
3.	Photograph of Crack Starting and Stringer Cope and Progressing into Web	3
4.	Photograph of Crack Through a Channel Constituting One Half of Built-up Chord of a Truss Bridge	5
5.	Photograph of Crack in Floorbeam Web Near the Connection to the Chord of the Tied Arch Bridge	5
6.	Photograph of Crack at the Attachment of Bearing to the Superstructure	7
7.	Photograph of the Truss Bridge for the South Bound Lanes of Interstate 5 Crossing the North Fork of the Lewis River	8
8.	Photograph of the Steel Tied Arch Bridge for the South Bound Lanes of Interstate 5 Crossing the Toutle River	8
9.	Locations of Cracking Noted for the Toutle River Bridge	9
10.	Locations of Cracking on the Lewis River Bridge	10
11.	S-N Curves Used in Fatigue Design of Steel Bridges	12
12.	Adaptation of AASHTO S-N Curves for Variable Amplitude Fatigue	14
13.	EUROCODE S-N Curves for Consideration of Variable Amplitude Fatigue	15
14.	Typical Stress History for Dynamic Truck Loading	16
15.	Rainflow Counting Method; a) Time History: b) Rainflow Counting	17
16.	HS-20 Truck Loads Applied in SAP90 Model	22
17.	Floorbeam End Rotation Modeling	24
18.	Side View of Interaction of Floorbeam, Chord and Vertical Member	24
19.	Mechanism of Measuring Rotation	26
20.	Member Response vs. Recorded Time	27
21.	Location and Type of Gauges on the Toutle River Bridge	28
22.	Location and Type of Gauges on the Lewis River Bridge	30
23.	WSDOT Truck Axle Spacing and Vehicle Mass	34
24.	Moment vs. Time, West Chord, Pass 1, Truck A, Toutle River Bridge	38
25.	Dynamic Amplification Due to Triangular Load Pulse	39
26.	Elevation of Interior Floorbeam of Lewis River Bridge	41
27.	Lewis River Bridge Interior Floorbeam Bending Moment, Truck A, Pass 3	43
28.	Stringer Neutral Axis Position, Truck A, Lewis River Bridge	46
29.	Stringer Neutral Axis Position, Truck A, Toutle River Bridge	46
30.	Moment and Neutral Axis Position for Stringer on Toutle River Bridge Due to Truck A Pass	47
31.	Measured Rotation	48
32.	Displacement, based on Acceleration Integration, Versus Time	50
33.	Stringer Stress Range versus Axle Weight (Toutle River Bridge)	51
34.	Floorbeam Flexural Stress Range versus Truck Weight (Toutle River Bridge)	53
35.	Chord Flexural Stress Range versus Truck Weight (Toutle River Bridge)	53
36.	Estimated Total Truck Load Spectrum for Toutle River Bridge	57

37. Estimated Total Truck Load Spectrum for Lewis River Bridge 57
38. Estimated Truck Axle Load Spectrum for Toutle River Bridge 59
39. Estimated Truck Axle Load Spectrum for Lewis River Bridge..... 59
40. Average Daily Traffic for Both Bridges 60
41. Estimated Fatigue Life for Cope Detail on the Toutle River Bridge 64
42. Estimated Fatigue Life for Cope Detail on the Lewis River Bridge. 64
43. Maximum Upperbound Fatigue Life Estimate for Cope Detail on the Lewis River Bridge 66
44. Sketch of Typical Built-up Floorbeams on Lewis River Bridge 68
45. Estimated Fatigue Life of Floorbeam at the Second Coverplate Termination on the Lewis River Bridge 68
46. Fatigue Life Predictions for the Most Severe Connection in the Bridge Truss of the Lewis River Bridge 70
47. Fatigue Life Prediction for Tie Chord of the Toutle River Bridge ... 71
48. Deflected Shape of Chord of Toutle River Bridge with Relationship to Truck Position; a) Truck at One Quarter Point; b) Truck at the Three Quarter Point 73
49. Local Deformation in Floorbeam Web at Floorbeam to Chord Connection 75
50. Possible Stiffening Method for Tied Arch Bridge 85
51. Possible Modification at Stringer to Floorbeam Connection 85

LIST OF TABLES

Table		Page
1.	Pass Description for the Toutle River Bridge	35
2.	Pass Description for the Lewis River Bridge	36
3.	Stringer Rotation Spring Flexibility Ratio	49

EXECUTIVE SUMMARY

Riveted steel truss and tied arch bridges in Washington state have experienced significant cracking that is due to fatigue loading. The Lewis River and Toutle River bridges are good examples of these two bridge types. They are both on the southbound lanes of Interstate 5 and experience heavy truck traffic. This research study addressed the fatigue cracking on these two bridges.

The cracking on these two bridges was summarized and analyzed. Computer models of the two bridges were developed, and static and dynamic analyses of the bridges were performed. These analyses provided a picture of the bridge behavior, and the results were combined with the observed damage patterns to develop instrumentation plans for both bridges. Strain gages, accelerometers, and potentiometers were installed on both bridges in the summer of 1996. Controlled load and weight station tests were performed on the two bridges with trucks of known weight and geometry traveling at known speeds and in known driving lanes. The results of these measurements were used to evaluate the overall behavior of the two bridges and to calibrate the instruments for further testing with trucks of unknown weight and geometry.

Upon completion of the calibration tests, uncontrolled truck traffic was measured for the two bridges over a period of 3 to 4 weeks. Extensive data were obtained for the two bridges, and load spectra were developed. These were combined with historic truck traffic data and predictions for future traffic in the I-5 corridor, and fatigue was estimated for critical components of the two bridges.

The Toutle River bridge was found to be very sensitive to dynamic vibration under truck loading, and fatigue cracking noted in the floorbeams of this bridge was found to be deformation driven. There is also a potential for stress driven fatigue cracking in the tie chord in coming years.

The Lewis River bridge was found to have serious fatigue cracking potential in the copes of the stringers for the deck system. There is less serious potential for fatigue cracking at the cover plate terminations of the floorbeams. There appears to be little potential for fatigue cracking in the truss members, unless there is an extreme nonuniform distribution of stress through the built-up members.

The ramifications of the fatigue cracking and possible repairs and modifications were evaluated.

INTRODUCTION

RESEARCH OBJECTIVES

The Washington State Department of Transportation (WSDOT) owns seven steel tied-arch bridges and more than 150 steel truss bridges. These bridges are typically of riveted construction, and they usually cross major rivers as part of major state highway or the Interstate systems. As a result, these bridges are important to the state and its economy. In recent years cracking has been noted on all of the tied arch bridges and approximately 15 percent of the steel truss bridges. Attempts have been made to repair the cracking, but these attempts have not always been effective. This research project examined this cracking problem. The objectives of the study were as follows:

- to better understand the cracking behavior and to establish the causes of cracking
- to determine the vibration characteristics of the tied-arch bridges and to establish the relationship of this vibration to the fatigue cracking
- to determine the range of dynamic loading due to truck traffic on critical elements of steel truss and tied-arch bridges
- to establish the effectiveness of existing repair methods and to propose new methods for repairing the fatigue damage
- to estimate the remaining fatigue life in critical elements of truss and tied-arch bridges on the basis of the best available information on the S-N curves for riveted bridge details.

THE PROBLEM

Steel tied-arch bridges and steel truss bridges in Washington State are usually of riveted construction, but welded and bolted construction are also occasionally employed. Significant fatigue cracking has been observed in riveted steel bridges in other states, but fatigue has not been regarded as a serious safety issue on riveted bridges because of the

locations of cracking and the relatively slow crack growth. Riveted steel truss bridges commonly have floorbeams that are transverse to the truss, as illustrated in Figure 1, and stringers that connect to the floor beams and are longitudinal to the truss, as shown in the figure. The stringer to floorbeam connections are normally created by coped web angle connections, as illustrated in Figure 2a, or by stiffened seat type connections, as illustrated in Figure 2b. Both of these connections were designed to be pin connections, but today they are regarded as partially restrained (PR) connections because they are known to have limited rotational restraint. Fatigue cracks have been noted at many of these stringer to floor beam connections. Most of these cracks have initiated near the corner of the cope and have progressed down into the web of the beam, as shown in Figure 3. Holes have been drilled through the tip of the crack to inhibit further crack growth. In connections with

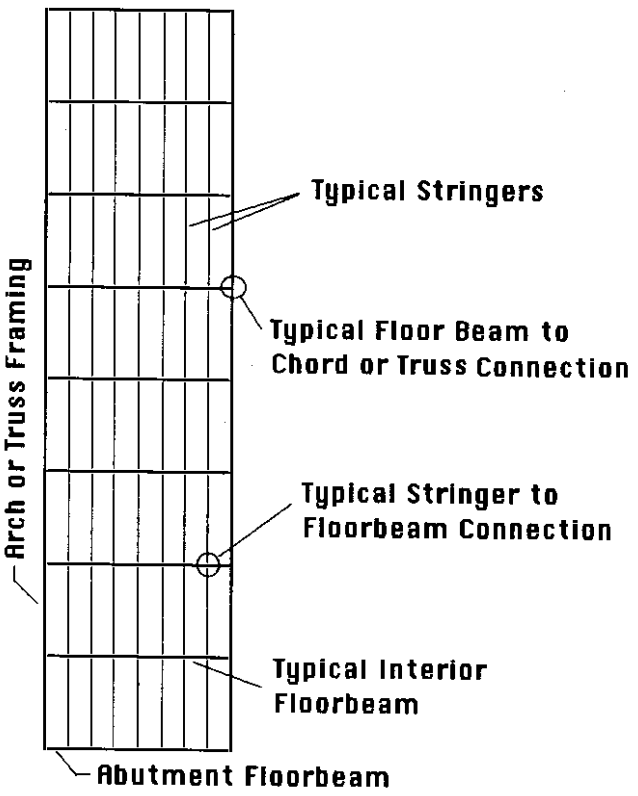

Figure 1. Typical Layout of Structural System for the Deck of Steel Truss and Tied-arch Bridges

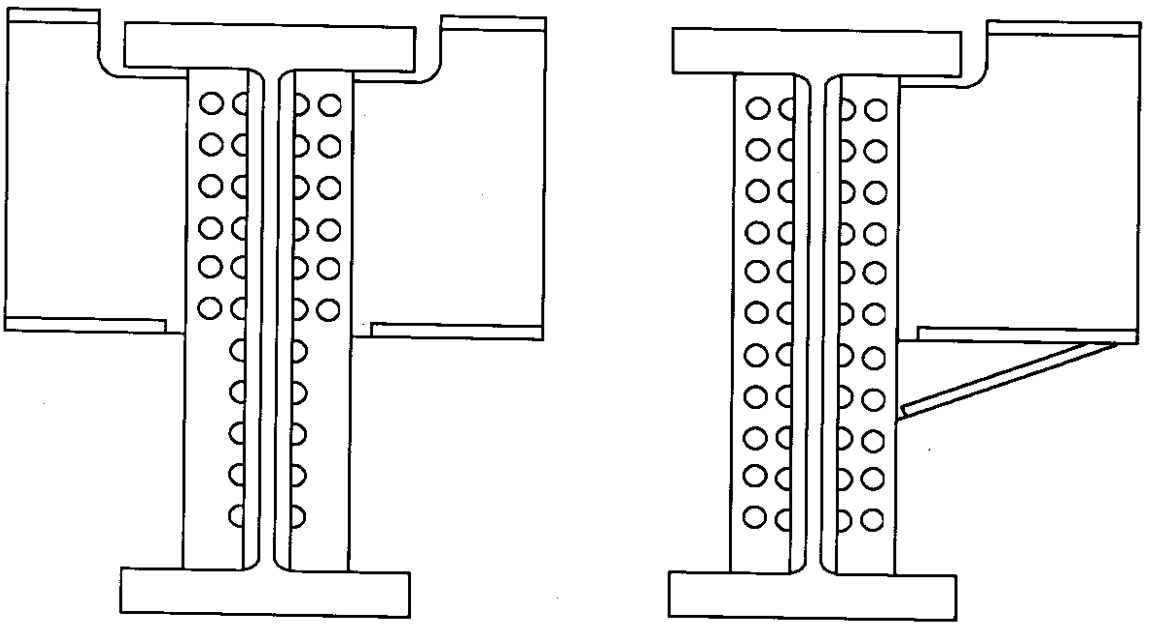

a) Coped Web Angle Connection

b) Stiffened Seat Connection

Figure 2. Typical Stringer to Floor Beam Connections

Figure 3. Crack Starting at Stringer Cope and Progressing into Web

larger cracks, bolts have been placed in the holes with or without clamping plates, and they have been tightened to induce a compressive stress at any potential crack tip to reduce the potential for further cracking. Other stringer to floorbeam connections have sustained cracking through the web angle, but this is not the most common crack location for these structural details.

The connections of the floorbeam to the truss chord and hangers have been designed as pinned connections. These connections have rotational restraint, and cracking in the floorbeam and the connection has been noted in some cases. However, this mode of cracking is less common for WSDOT bridges than the stringer cope cracking described earlier. Deck system cracking in truss bridges has been occurring with increasing frequency on an increasing number of bridges in recent years. However, the inspection reports suggest that the hole drilling repair methods are at least temporarily controlling further crack growth for the stringer cope connections.

To date one major truss bridge has experienced chord cracking, as illustrated in Figure 4. This cracking has occurred infrequently, but it represents a very serious concern because there is no redundancy within the structure and no means of supporting gravity loads if these members fail.

Similarly, cracking has been noted in the tied-arch bridges. Tied-arch bridges have deck system members and connection details similar to those of the truss bridges, and the tied-arch deck system is also illustrated in Figure 1. As a result, similar fatigue cracking has been noted. However, there are two significant differences between the steel tied-arch behavior and steel truss bridge behavior. First, several different modes of cracking have been noted. The tied-arch bridges have most commonly developed cracks in the floorbeams near the floorbeam-to-chord connection. The cracks grow approximately horizontally through the web of the floor beam near the top flange of the floorbeam at the chord connections, as shown in Figure 5. Holes have been drilled through the tips of these

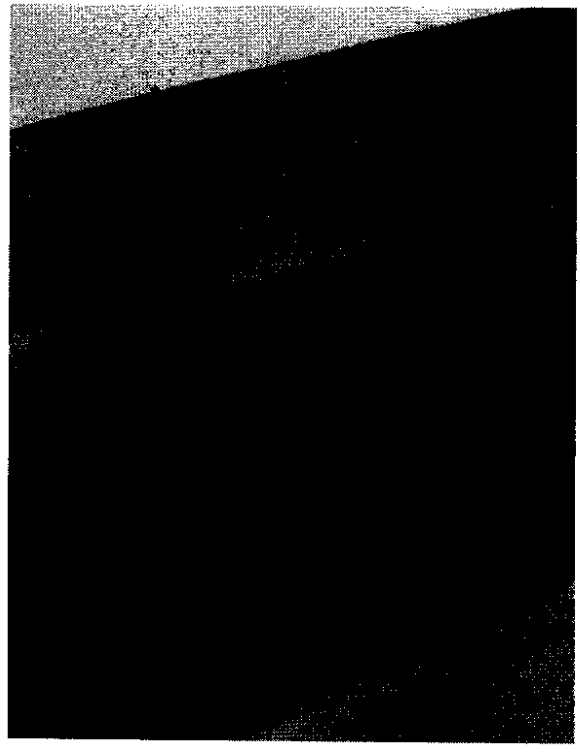

Figure 4. Crack Through a Channel Constituting One Half of the Built-up Chord of a Truss Bridge

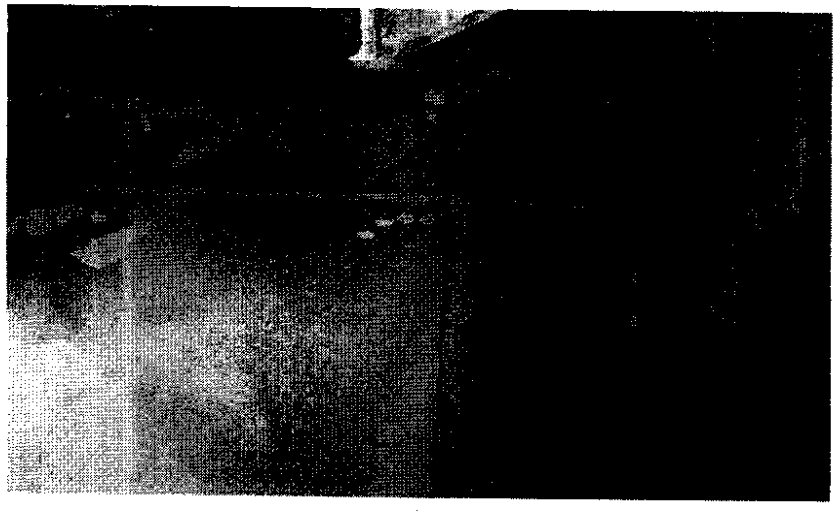

Figure 5. Crack in Floorbeam Web near the Connection to the Chord of a Tied-Arch Bridge

cracks to stop the cracking, but the hole drilling technique has generally been ineffective because many holes have been drilled without stopping the crack, as shown in the figure. Another repair technique has employed a bolted flange plate between the top flange of the floor beam and the top flange of the chord to restrain relative movement between these two elements. This has slowed the crack growth at the floorbeam to chord connection, but it has driven cracking to other locations. Cracks are now being noted in the web of the floorbeams near the stringer-to-floorbeam connections. The progression of the crack locations is a serious concern.

A second major difference between the tied-arch bridges and the truss bridges is that all of the tied-arch bridges in Washington State exhibit significant vibration to truck traffic. This vibration is easily felt by a pedestrian on the bridges, and deflections can easily be seen by an observer watching the bridge under truck traffic. The truss bridges do not exhibit these extreme vibration characteristics, and there is concern that the difference in the dynamic response may be a contributing factor in the cracking noted on the tied-arch structures.

One final issue requires some discussion. A number of the tied-arch and truss bridges that have sustained fatigue have also experienced cracking where the bearings are attached to the superstructure. Figure 6 is a photograph of one such crack. This cracking also raises questions about whether there is a relationship between this cracking and the damage noted elsewhere in the structure.

SPECIFIC ISSUES

This research studied the cracking problems observed in many bridges in the state of Washington. The study was a field study, since it evaluated the loads, stresses, and deformations actually occurring in the bridges under normal truck traffic. However, it was impossible to perform fatigue evaluation of all of the bridges experiencing this cracking in the state. The cost of field testing, combined with the time required to complete the work, restricted the field measurements to two bridges. The bridges were selected on the basis of

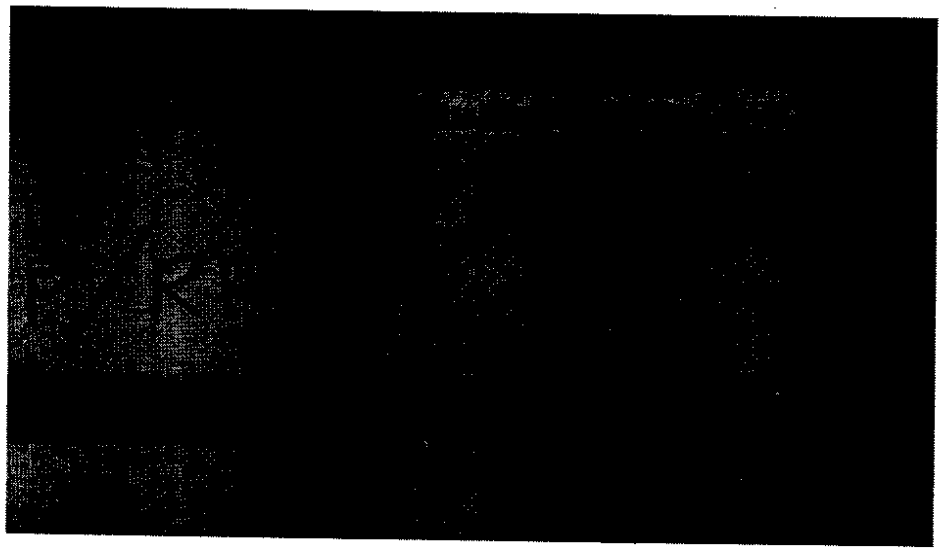

Figure 6. Crack at the Attachment of Bearing to the Superstructure

numerous considerations. First, the two bridges had to reflect the variations in behavior expected for both steel tied-arch and truss bridges throughout the state. Second, the selected bridges had to display the range of cracking behavior noted in these bridges in recent years. Third, the selected bridges had to be heavily used by truck traffic, as is typical for these bridges in Washington State. Last and foremost, the selected bridges needed to be readily accessible to the researchers so that measurements could be taken without interfering with traffic and without placing the research team at risk.

The two bridges selected were the west (southbound), three-span, continuous steel truss bridge crossing the North Fork of the Lewis River, as shown in Figure 7, and the west (southbound), tied-arch bridge crossing the Toutle River, as shown in Figure 8. They were approximately 50 km apart, and both bridges were in the southbound lanes of I-5. This assured that the two bridges would have similar truck traffic and were close enough that interaction and communication between the researchers working on the two bridges would be feasible. At the same time, all modes of cracking described earlier, except the chord cracking illustrated in Figure 4, were seen on these two bridges, and they also clearly illustrated the differences between the tied-arch and truss bridge behavior.

Figure 7. Truss Bridge for the Southbound Lanes of Interstate 5 Crossing the North Fork of the Lewis River

Figure 8. Steel Tied-Arch Bridge for the Southbound Lanes of Interstate 5 Crossing the Toutle River

The Toutle River Bridge is 92.66 m long, with 11 bays in the arch and floor system. Each bay of the floor framing has seven stringers, which are 2.29 m on center and have shear connectors distributed over their length. The arches are 16.75 m apart center to

center. There is no skew in the structure, and the arch and deck system are symmetric. The north end is pinned, and the south end is movable. The bridge is known to be flexible and lively under truck traffic, and fatigue cracking of the floorbeam web at the floorbeam-to-chord connection has occurred at all interior floorbeam connections. This type of cracking is illustrated in Figure 5. In addition, three of the web angles at these same floorbeam-to-chord connections have exhibited cracking. In 1989, these floorbeam to chord connections were repaired. The top flanges of the floorbeams were connected to the top flange of the chord by a flange plate to eliminate distortion of the connection. Since that date, crack initiation has moved down the web of the floorbeam at the stringer-to-floorbeam connection.

In the abutment floorbeams of the Toutle River Bridge, the abutment floorbeam was directly connected to the chord from the original construction with a flange plate. Two of these riveted flange plates have experienced serious fatigue cracking and have required replacement. Figure 9 illustrates the locations of cracking noted in the Toutle River Bridge.

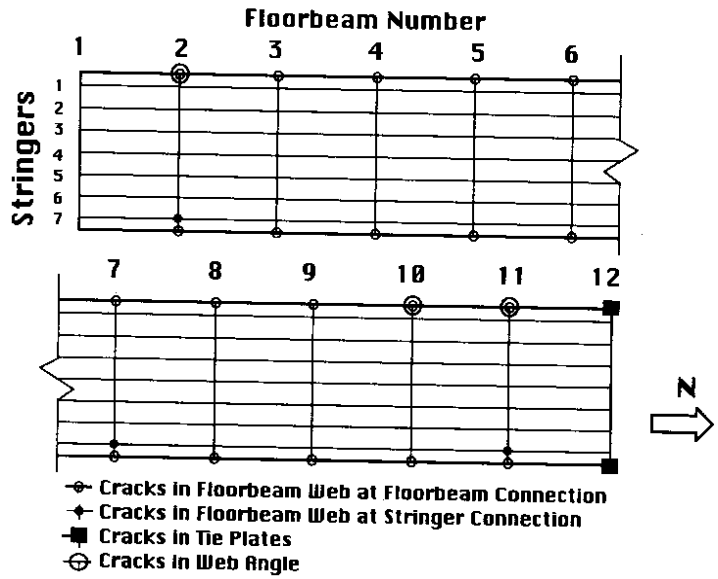

Figure 9. Locations of Cracking Noted for the Toutle River Bridge

The Lewis River Bridge is 246.9 m long, with 30 bays in the truss and floor system. Each bay of floor framing has nine stringers, which are 1.777 m on center. The trusses are 15.55 m apart center to center, and the bridge deck has no skew with respect to the abutments and the longitudinal axis. However, the two interior piers are sharply skewed at a skew angle of approximately 43.4° between the longitudinal axis of the bridge and the axis of the internal piers. The result of this internal skew means that the deck system is symmetric, but there is a substantial asymmetry in the truss system. The south end of the bridge is pinned, and the interior piers and north abutment are movable. Fatigue cracking, as illustrated in Figure 3, has been noted at the stringer to floor beam connections at 14 locations of the bridge deck. Most of these locations are in the second or third stringers from the west side of the bridge under the right hand driving lane. Figure 10 illustrates the locations of cracking noted for the Lewis River Bridge.

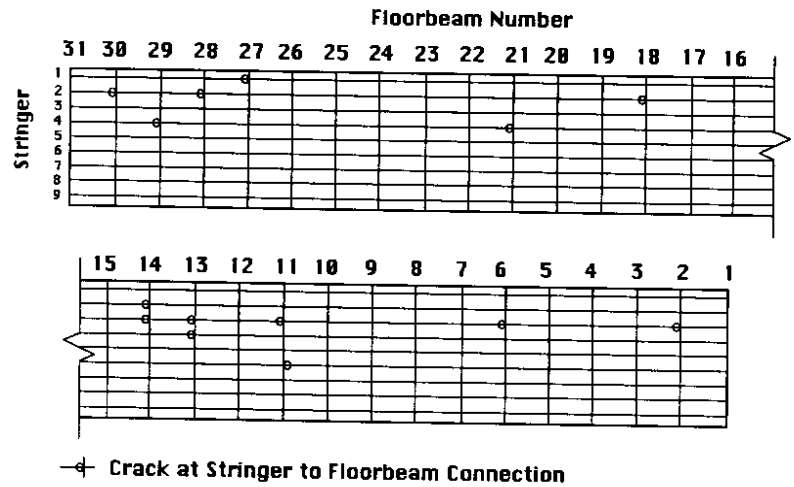

Figure 10. Locations of Cracking on the Lewis River Bridge

REVIEW OF CURRENT PRACTICE

LITERATURE REVIEW

Engineers building steel bridges before 1974 gave little or no consideration to fatigue. Fatigue design provisions as we know them today were first introduced into the American Association of State Highway and Transportation Officials (AASHTO) Standard Specifications for Highway Bridge in the early 1970s (AASHTO 1973). Before this date, stresses due to alternating or cyclic loads were checked against a stress limit obtained from a modified Goodman procedure (Frost et. al. 1974). This earlier procedure may have reasonably estimated the fatigue performance of plain steel members, but it did not account for the effect of imperfections introduced by welding, fabrication, and connections. The fatigue design procedure, which appears in the 1973 AASHTO Standard Specifications, was developed in response to fatigue cracking observed in bridges built before this period and research performed on welded specimens (Fisher et al. 1970, and Fisher 1984). The design procedure was an extension of methods that had earlier been developed for railroad bridges and other welded structures. With this method a series of S-N curves, as shown in Figure 11, are used to establish the limit on the stress range as a function of the number of cycles of loading. These S-N curves establish a relationship between the stress range and the number of cycles that can be tolerated at that stress level. In design specifications, simple sketches of the geometry of the detail and the load characteristics are correlated to the different S-N curves and fatigue categories. The different S-N curves represent different severities of the fatigue detail, and the individual curves are matched to specific details on the basis of constant amplitude fatigue test results or field observations of the behavior of the detail in question. These S-N curves show that the allowable stress range depends upon the number of cycles of loading, but they also suggest that an infinite fatigue life is possible if the stress is always maintained below the fatigue limit. The S-N curves shown in Figure 11 are selected on the basis of constant amplitude fatigue test results, and

the goal is that they lie approximately two standard deviations on the conservative side of the mean for fatigue fracture. These curves are normally applied to redundant structures, which are unlikely to fail if a fatigue fracture occurs. The S-N curves are revised for nonredundant components. For these nonredundant elements, the allowable stress range is reduced to 80 percent of that permitted for redundant elements at the same number of cycles.

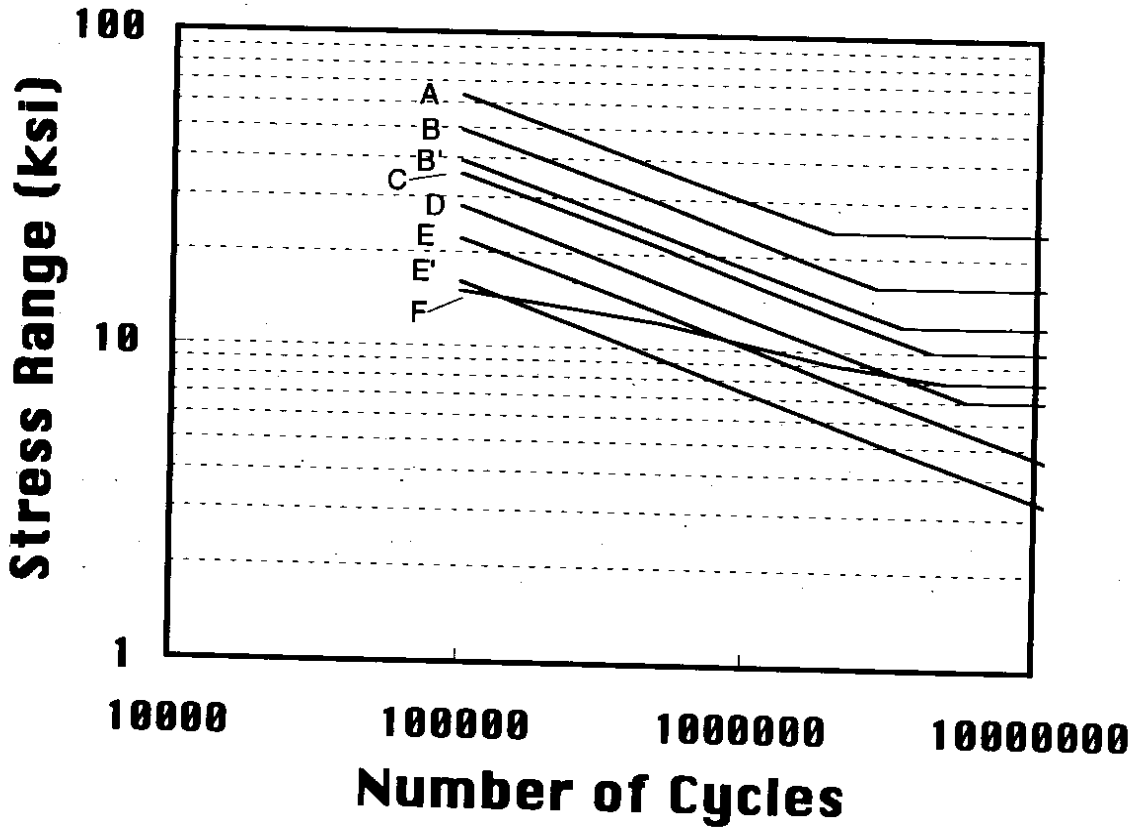

Figure 11. S-N Curves Used in the Fatigue Design of Steel Bridges

The computed stress range historically used in this AASHTO fatigue design procedure is the stress associated with an HS20-44 truck, and under normal bridge design AASHTO requires that the computed stress range be limited to assure that more than 2 million cycles of this standard truck loading can be supported by the bridge. This simplified design procedure has been used to design many bridges and is still used in design practice. However, this is not a good indicator of actual bridge behavior, and

therefore it is not a good tool for evaluating the expected fatigue life of existing bridges. First, the stress range provided by the HS20 vehicle is arbitrarily large in comparison to most trucks, whereas the 2 million cycles of truck loading is very small in comparison to the number of trucks crossing the typical steel highway bridge. As a result, further study was instituted to examine the fatigue life of bridges under variable amplitude loading (Schilling et al. 1978).

Various studies have suggested that Miner's rule (Miner 1945) is a satisfactory way of establishing an average or equivalent design stress that reflects the full range of the variable amplitude truck loading history. With this method, the fatigue life is defined by

$$\sum \frac{n_i}{N_i} = 1 \qquad \text{(Equation 1)}$$

where n_i is the number of cycles actually sustained at a given stress level, and N_i is the number of cycles permitted at that given stress level. This model requires knowledge of the actual load history rather than an arbitrary design value, and as a result, research has been performed to better understand and generalize the statistical variation of highway bridge loading (Moses et al. 1987, and Novak 1992). Today, evaluation of the fatigue life of existing bridges normally requires a measurement or assessment of truck traffic (or corresponding stress ranges produced by that traffic) to fully consider the expected fatigue life.

Although Miner's rule is the best available method for assessing fatigue caused by variable amplitude loading, it is clearly not precise in that considerable variation has been noted when results from this model have been correlated to the results from variable amplitude experiments. As a result, further modifications have been made to the basic fatigue design procedure to permit its use in evaluating the fatigue life of existing structures. First, it is has been noted that the fatigue limit of the S-N curve is different for variable amplitude fatigue than for constant amplitude fatigue. The fatigue or endurance limit does not appear to be as clearly defined for variable amplitude fatigue as for constant amplitude fatigue, and stress cycles, which are much lower than this limit, may contribute

to fatigue behavior if one or more earlier stress cycles are larger than the constant amplitude fatigue limit. Two different methods have evolved for dealing with this difference. In the US, the S-N curve for each category of fatigue behavior has been modified, as illustrated in Figure 12. With this modified method, the normal sloped S-N curve is extended below the constant amplitude fatigue limit, as shown in the figure, and this sloped portion of the curve is used in the Miner's rule accumulation of fatigue effects if at least one earlier cycle exceeded the constant amplitude fatigue limit. The S-N curves and fatigue design practice used in Europe historically have been similar to US practice, but the effect of variable amplitude fatigue on the fatigue limit is handled differently in the EUROCODE, as illustrated in Figure 13. This European method employs the same basic S-N curve, with a slope of - 1/3 in the log-log curve until the constant amplitude fatigue limit is encountered.

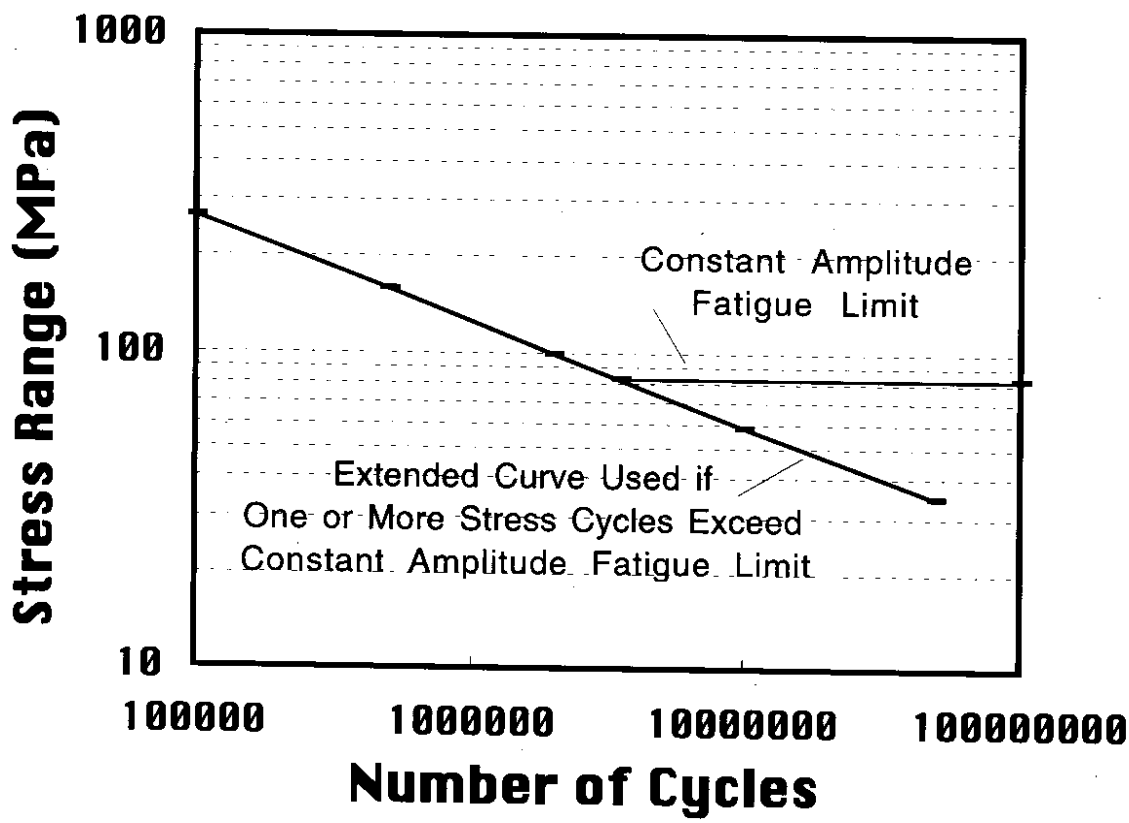

Figure 12. Adaptation of AASHTO S-N Curves for Variable Amplitude Fatigue

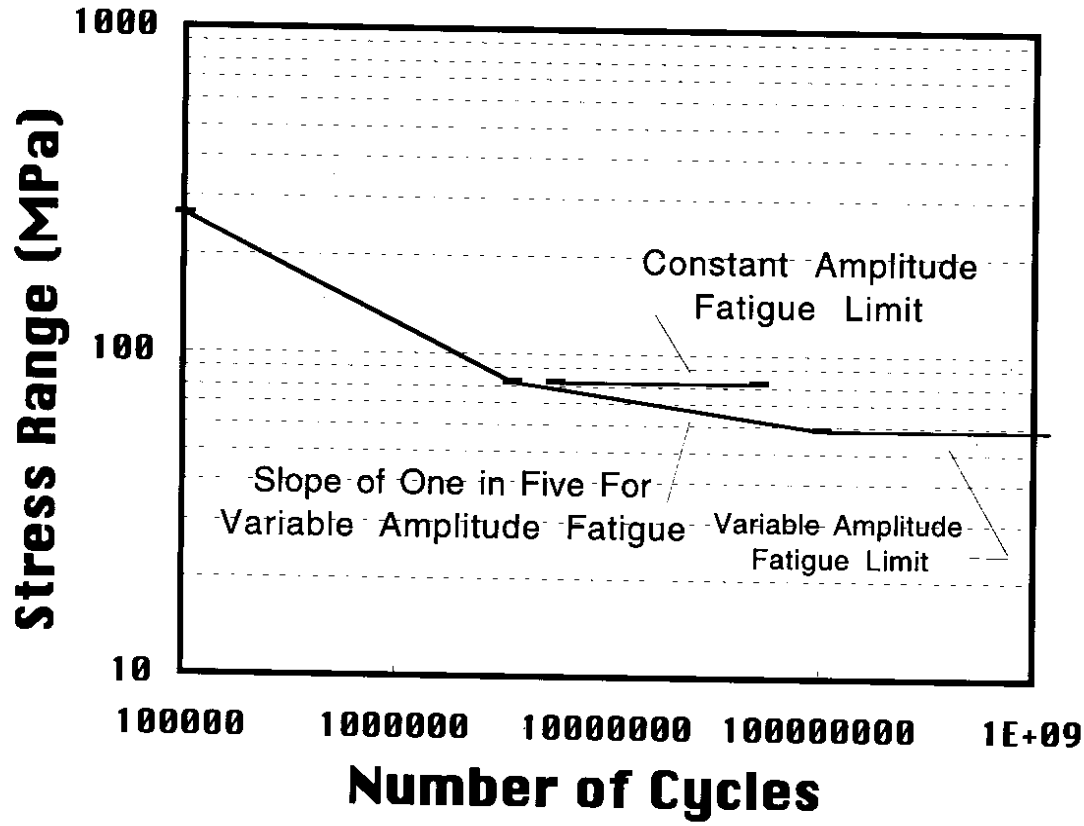

Figure 13. EUROCODE S-N Curves for Consideration of Variable Amplitude Fatigue

At this point a reduced slope (- 1/5) is used until approximately 100 million cycles, and the stress range associated with 100 million cycles is taken as the variable amplitude fatigue limit.

A second issue that requires special consideration for variable amplitude fatigue is the actual stress range values used in the fatigue evaluation. Figure 14 shows a typical time dependent variation of stress due to a dynamic truck loading on a bridge element. The stress range values and number of cycles are not uniquely defined with this realistic stress history. A consistent procedure is needed that permits a unique definition of the stress cycles while providing good correlation with constant amplitude S-N curves. The rainflow analysis method has been accepted as the best method for incorporating the wide variation of the stress time history produced by heavy truck traffic. This method is schematically

illustrated in Figure 15. The method permits the combination of the peak stresses achieved with different vehicles over the total history of the bridge, although practical limitations on data analysis hamper this capability. With this method, a stream is started at each peak and trough, as shown in the figure. The stream continues until the stress signal reverses direction. At this point the stream falls until it either encounters another stress signal or is the maximum value included in the stress history. If the falling stream intercepts another stream, the intercepted stream is terminated. If the falling stream does not intercept another stream, this falling point defines the limit on the maximum range encountered in the stress history. The stress ranges for all streams (including all of the interrupted streams) are included in the analysis, and these ranges are accumulated by a Miner's rule formulation. While this procedure was developed for other applications, it has come to be an accepted procedure for fatigue evaluation.

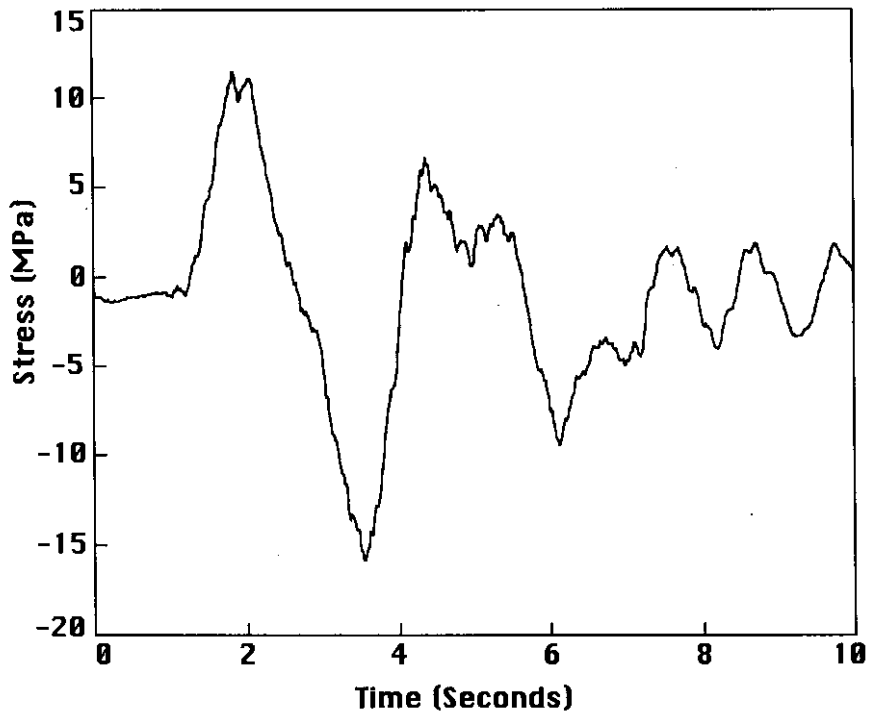

Figure 14. Typical Stress History for Dynamic Truck Loading

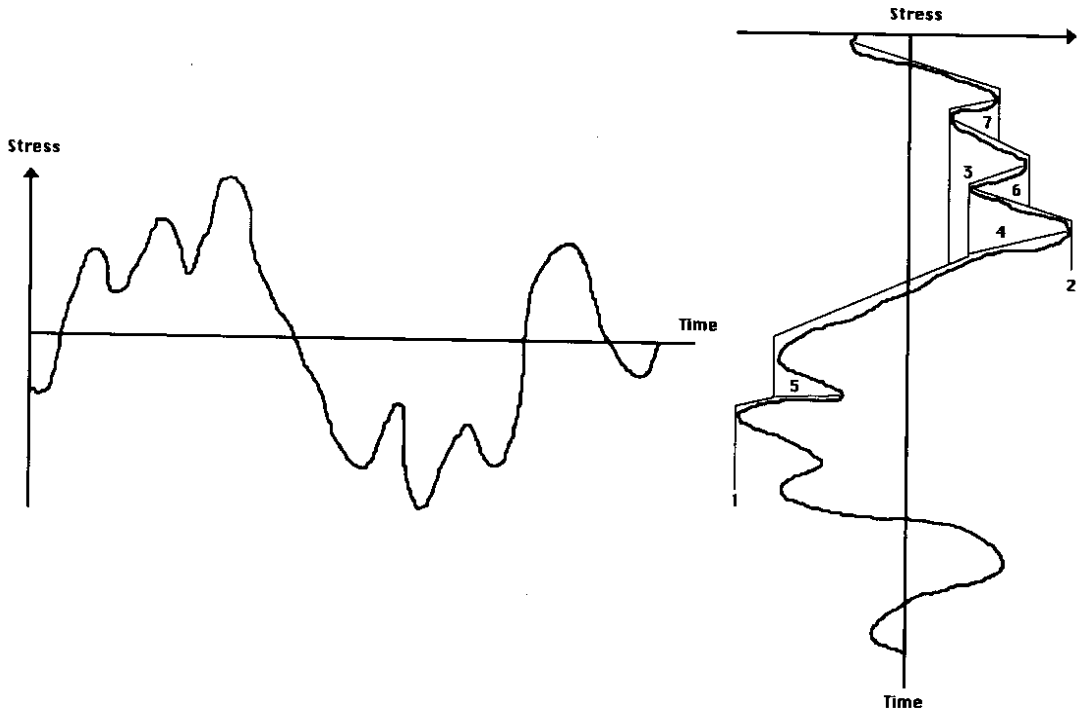

a) Time History b) Rainflow Counting

Figure 15. Rainflow Counting Method

Research has been performed to combine these issues and make realistic estimates of fatigue life (Moses et al. 1987). AASHTO guidelines (AASHTO 1990) have been developed to incorporate these efforts. However, despite these efforts, the application of these provisions to riveted truss and tied arch bridges still has serious limitations. First, information regarding the fatigue life of riveted connections and structures is limited. In general, riveted structures are not regarded as sensitive to fatigue, but very few tests have been performed. A limited series of fatigue tests on riveted connections have been performed (Fisher et al. 1987), and these tests suggested that fatigue Category D is a lower bound indicator of the initiation of cracking of riveted connections, whereas Category C is a lowerbound indicator of the total fatigue life. The Category D is viewed as an extremely conservative lower bound because this category is appropriate for tensile stress around an open hole. Rivets in good condition fill the hole and develop a clamping force that should

retard crack growth. Additional tests examined the fatigue characteristics of riveted members where rivets have been replaced by high strength friction bolts (Reemsnyder, 1975). The observed behavior indicates that this is an effective way of increasing the fatigue life of riveted connections. Very few riveted details have been tested for fatigue, but the coped beam with bolted connections has been tested (Yam and Cheng 1990). The results of these tests appear to be relevant to the riveted connections commonly used in the deck system of WSDOT riveted tied-arch and truss bridges. These results show that fatigue fracture may initiate from the cope of the beam section. In normal fatigue design calculations, nominal stresses are computed. However, the recommended method for addressing the fatigue of these coped connections requires that the stress concentration be estimated, since this mode of fatigue fracture is extremely sensitive to local curvature and cope roughness. When this stress concentration is estimated, Category C is viewed as the best indicator of the initiation of visible cracking, and Category B is accepted as the better indicator of fatigue life or fatigue fracture. This report contains the best available information on cope crack fatigue life, but the recommended approach is somewhat unusual and must be viewed with caution.

The fatigue evaluation procedures described to this point all are based upon a computed stress under a nominal truck loading, spectral loading, or an equivalent loading for a given load spectrum. These computed stresses are usually nominal stresses computed by elementary mechanics methods. In all cases these computed stresses are then compared to the permissible stress range for the required number of load cycles. However, research has shown that some fatigue problems cannot be addressed in this manner. These fatigue problems are commonly attributed to distortional fatigue (Fisher et al. 1990). That is, the fatigue cracks are driven by local distortions in the member. Clearly, there are stresses associated with this fatigue cracking, but they are not as easily calculated as normal fatigue stresses. As a result, this fatigue behavior falls into a separate class of behavior and is treated somewhat more heuristically than is the normal fatigue.

CORRELATION OF EXISTING KNOWLEDGE TO RIVETED BRIDGES

It is clear that great strides have been made in designing new bridges for fatigue, as well as in evaluating the remaining fatigue life of existing bridges. The AASHTO Guidelines (AASHTO 1990) are particularly useful for this second endeavor. However, there are also clear limitations in evaluating the fatigue life of older riveted steel bridges such as those considered in this study. These limitations can be divided into three major issues.

The first issue concerns accurate determination of the truck loads and stress ranges for the bridge in question. This information is essential for accurate evaluation of the remaining fatigue life for any bridge, and it requires field measurements of existing truck traffic to establish how many trucks are crossing the bridge within a given period and to establish fatigue stress ranges expected for these trucks. These field measurements are particularly important with older steel bridges because design methods have changed, and engineers have a less clear understanding of the stresses and stress states expected in these existing structures. This first issue was the primary focus of this research study.

The second issue is also a load-based issue in that deformation-based fatigue may occur in riveted structures, as well as in welded steel structures. The deformational fatigue is caused by large, local tensile stresses resulting from local deformation. However, it is not possible to compute these stresses so that they can be compared to S-N curves for evaluating fatigue life and the potential for fatigue cracking. Under these circumstances it is also difficult to predict whether cracks will grow to an unstable condition or stabilize after reaching an adequate size. This limitation also substantially limits the ability to predict the fatigue life of riveted structures.

The third issue hindering the estimation of fatigue life relates to the fatigue capacity side of the equation. S-N curves are commonly used to establish the fatigue capacity of alternative structural details and configurations. These S-N curves are invariably based upon extensive laboratory testing of large-scale specimens under constant amplitude fatigue

conditions. Generally, engineers believe that riveted structures are less sensitive to fatigue than welded structures, and clearly the existing life of the Lewis River Bridge, Toutle River Bridge, and other similar structures support this conviction. However, recent experience has shown that fatigue ultimately is a potentially serious problem for riveted steel bridges, and beyond the 14 riveted girder tests performed by Fisher (Fisher et al. 1987), no laboratory test data are available to establish the S-N curves for riveted structures or for the repairs and modifications that may be applied to them. This third issue is beyond the scope and funding of this research project. Fatigue life estimates were made as part of this research study, but they were inherently approximate because they were based on rough inferences of fatigue life based on limited knowledge.

BRIDGE MODELING AND PREDICTED GLOBAL BEHAVIOR

Computer analyses were performed to begin to understand the bridge behavior and to prepare for the experimental work. The elastic 3-D computer program SAP-90 (Wilson and Habibullah 1995) was used to model the bridges. Global bridge behavior and the floor system behavior were modeled separately. Modal and time history analysis were used to identify natural periods of the bridges, to obtain the predicted response due to truck loading, and to identify members for instrumentation.

In the global analysis, frame elements were used for all members and floorbeams. Member models were simplifications of the actual members, which changed properties many times along their length. All connections were assumed to be fully restrained (FR). Clearly, most of the riveted connections were partially restrained (PR), with various degrees of end restraint. The rigid assumption was found to have only a small effect on the in-plane behavior of the truss and arch systems, but it produced relatively large out-of-plane bending effects in the hangers of the Lewis River bridge. As a consequence, these bending effects were an issue of concern in the experimental investigation. Hangers on the Toutle River bridge were assumed to carry no moment. Stringers were not included in the models for simplicity, but floorbeams, truss, and arch cross-bracing and diaphragm stiffness of the deck were included. Four-node concrete deck slab elements were assumed to be pinned to the floorbeams at their ends to provide diaphragm stiffness and deck mass.

A load representative of an HS-20 truck (AASHTO 1996) with axle weights of 35.6kN, 142kN, and 142kN spaced at 4.3m was applied to the floorbeams, as shown in Figure 16. The load pattern applied from each axle on a floorbeam was a triangular function with time as a truck travelled over the bridge. The number of axles contributing

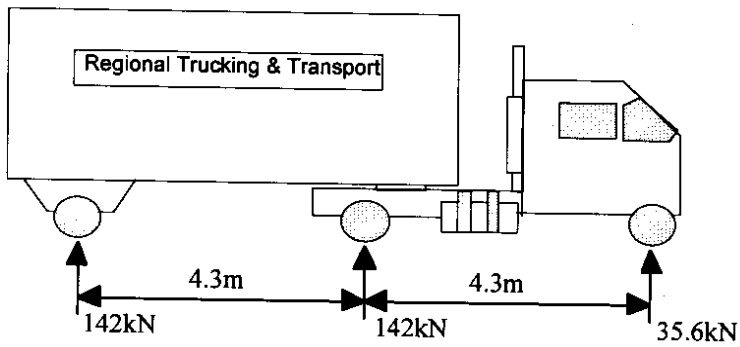

Figure 16. HS-20 truck loads applied in SAP90 model

to the floorbeam load at any time was considered in the analysis (Wong 1997). Total load on all of the floorbeams was at all times equal to the weight of the truck. The rate at which the loading moved over the bridge was related to the assumed truck speed. The applied loading position on a floorbeam was determined from the lane in which the truck was assumed to travel. The right hand (west) lane was used to obtain the peak stresses on the west truss/arch. The effect of truck mass, as well as surface roughness and suspension system effects, on the overall response of the bridge was ignored.

For the Lewis River bridge, periods of the first 40 modes of vibration ranged from 0.476s to 0.264s. These modes represented a total mass participation of 90 percent in the longitudinal direction, 72 percent in the vertical direction, and 72 percent in the lateral direction. Dynamic truck loading gave a peak axial stress range of approximately 10.3MPa in the top chord and diagonal members. Strong-axis (in-plane) bending stresses were generally less than 3.5MPa. Out-of-plane bending stresses as high as 62MPa were predicted in the vertical truss members at the floorbeam connections. These stresses were considered to be unrealistically high because line elements of no depth were used to model members with finite depth, and FR connections were assumed. The stresses changed by less than 2 percent as a result of trucks assumed to travel at 96.5km/h rather than 9.65km/h.

For the Toutle River bridge, periods of the first 20 modes of vibration ranged from 1.08s to 0.27s. The first mode shape approximated a full vertical sine wave of the

chords and arches over the length of the bridge. The participation factor for vertical movement was low, at 0.88 percent, because of the asymmetric mode of vibration. However, this mode provided the bulk of the response for dynamic response calculations. Dynamic truck loading gave peak axial stress ranges as high as 43MPa (6.3ksi) in the chord and 24MPa (3.5ksi) in the arch at one quarter of the span length from each end. Displacements at these points ranged from 23mm up, when the truck was on the far side of the bridge, to 29mm down, when the truck was over the point considered. The total displacement range due to one HS-20 truck was thus 52mm.

PREDICTED LOCAL BEHAVIOR

Local modelling of the floorbeams and chords was carried out to determine the rotation of the ends of the floorbeam caused by the stiffness of the chord and any other members at the end of the beam. The total rotation at the end of a floorbeam is determined by the connection flexibility, as well as by the rotation described above.

For the Toutle River Bridge, the chord at the floorbeam connection was assumed to resist rotation by torsion. Chord torsion was assumed to occur over two bays of the bridge, and no torsional rotation was permitted at the floorbeam-chord connection on either side of the floorbeam being investigated. This is reasonable if a short truck crosses the bridge, but the assumption was also used for longer trucks, which may have been less valid. The total rotational restraint at the floorbeam ends was modelled as a rotational spring of stiffness k_r at either end, as shown in Figure 17. The value of k_r was calculated as approximately 226,000kNm/rad for the interior floorbeams. The end restraint was probably greater than this in the exterior floorbeams because of the additional restraint of the arch and the out-of-plane restraint of the bearing.

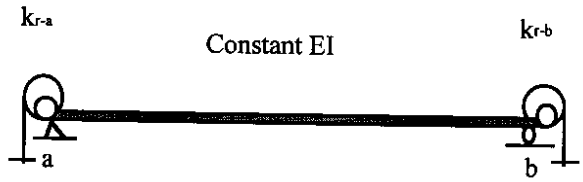

Figure 17. Floorbeam End Restraint Modeling

For the Lewis River bridge, the vertical hangers as well as the chord provided some rotational restraint at the end of the floorbeam, as shown in Figure 18. The top of the vertical member was assumed to have a pinned connection. The restraint provided by the chord was ignored because its torsional stiffness was much less than the box section on the Toutle River Bridge. The rotational stiffness, k_r, was calculated as approximately 22,600kNm/rad on the basis of the bending stiffness of the hanger. For the abutment, or exterior, floorbeams, k_r was difficult to quantify because of an expansion joint out-of-plane rotational restraint of the bearing and multiple members framing together at the ends of this beam.

Fundamental frequencies for Toutle River Bridge interior floorbeams and stringers were computed as 0.086s and 0.053s, respectively. They were 0.159s and

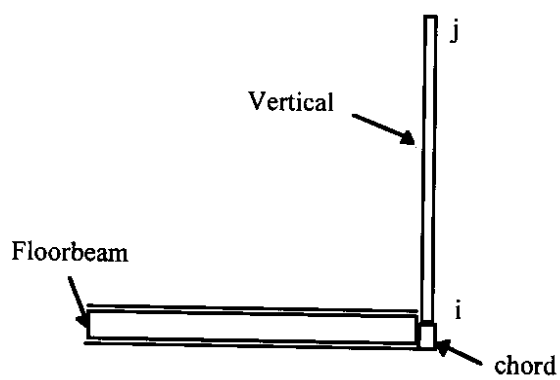

Figure 18. Side View of Interaction of Floorbeam, Chord and Vertical Members in Lewis River Bridge

0.037s, respectively, for the Lewis River Bridge (Arima 1997). The end restraint obtained from the methods described above, with no composite action, was used in these calculations.

INSTRUMENTATION

Instrumentation was placed on the Toutle and Lewis River bridges so that the global bridge behavior could be captured, analytical modelling parameters for assessing the bridge performance could be calibrated and loading spectra due to normal traffic could be determined.

Members selected to be instrumented were required to meet the following criteria. First, the stress ranges obtained in the analysis had to be large enough to provide meaningful readings. Second, a range of different member types, including stringers, floorbeams, and chords, measuring different aspects of bridge response and the full range of member behavior had to be selected. Third, instrumentation locations had to be close to the ends of the bridges where the data acquisition systems were set up, since this simplified installation and reduced signal noise.

Instrumentation consisted of strain gauges, linear potentiometers, and accelerometers. *Strain gauges* with 350 ohm resistance were placed in full-bridge configurations to measure either curvature or axial strain. This configuration automatically compensated for strain due to temperature. Methods of obtaining strain or curvature from the voltage output of the gauges are given by Wong (1997). *Linear potentiometers* with 12.7mm stroke were used to measure rotation at the ends of the stringers relative to the floorbeams. The device is shown in Figure 19. The top plate was fastened with C-clamps onto the bottom flange of the stringer, and the potentiometers measured displacement with respect to the floorbeam web. Rotation was computed from the relative movement of the potentiometers. This measured rotation included twist of

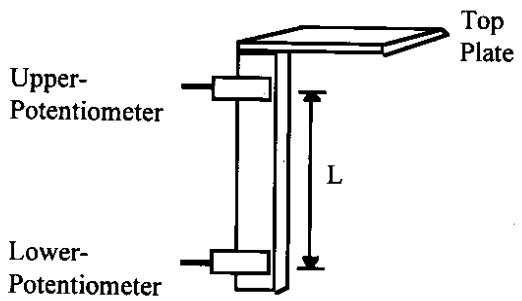

Figure 19. Mechanism of Measuring Rotation

the floorbeam web, as well as end rotation of the stringer. *Accelerometers* were also used on the Toutle River bridge to indirectly measure absolute bridge displacement. It was not possible to measure the vertical deflection of the bridge relative to the ground directly, and so the signal from the accelerometers was integrated twice.

Data acquisition was carried out with 166MHz Pentium computers that had 2GB of disk storage. Strain gauge and accelerometer data were amplified by a strain gauge conditioner before being fed into one of the two 16-channel, 16-bit A-D converter boards at each bridge site. Linear potentiometer signals were sent into the other A-D converter board. Signals from the A-D boards were recorded with the Labtech Notebook-Pro version 9.0 (Putnam 1996) software, scaled, and stored on the computer disk. Channels were nulled daily by hand to compensate for drift and to avoid an extreme imbalance.

Data were monitored continuously by the computer, and they were stored to disk when the board had been triggered. Two types of triggering were used, *manual triggering* and *automatic triggering*. *Manual triggering* was used to record the bridge response due to specified trucks in the "controlled loading" tests. *Automatic triggering* was used to record truck response during normal traffic over a period of several weeks. When the signal at a specified gage or accelerometer exceeded a threshold, data were written to the disk for a period of time. The threshold was set to record every heavy truck that passed over the bridge. Data were written to disk for periods ranging from 7s to 10s.

These periods were determined from controlled loading test measurements to record the majority of the response of each truck. Some of the time before the trigger was activated, shown as the "pre-trigger period" in Figure 20, was also written to disk with one of the features of the software. The pre-trigger period was used to capture smaller amplitude response as the truck entered the bridge, and it was adjusted according to bridge geometry and traffic. A maximum recording speed of 200Hz per channel was used in the initial runs. This was later changed to 100Hz, which was found to provide sufficient accuracy.

The locations of strain gauges and potentiometers placed on the Toutle River bridge are shown in Figure 21. Strain gauges were used to measure curvature on the two stringers at the west side of the bridge in the truss south bay. Measurements were taken at mid-span and at a distance of 2/3 of the stringer length from the south abutment. Curvature was also measured at two locations on the abutment floorbeam and the floorbeam north of the abutment floorbeam, as shown in Figure 21. Curvature was measured near the ends of the floorbeams at these positions because larger strains were expected here rather than at the mid-span of the floorbeam. This was indicated by the reduced section size at this position and because one of these gages was directly under the right-hand lane of traffic. Axial strain was measured by strain gages at the mid-span

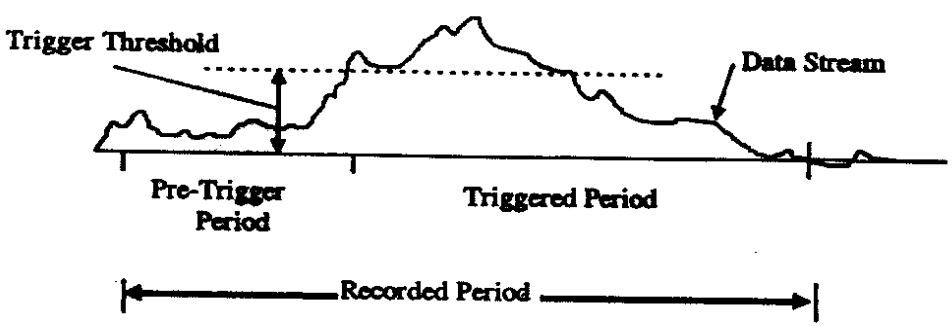

Figure 20. Member Response vs. Recorded Time

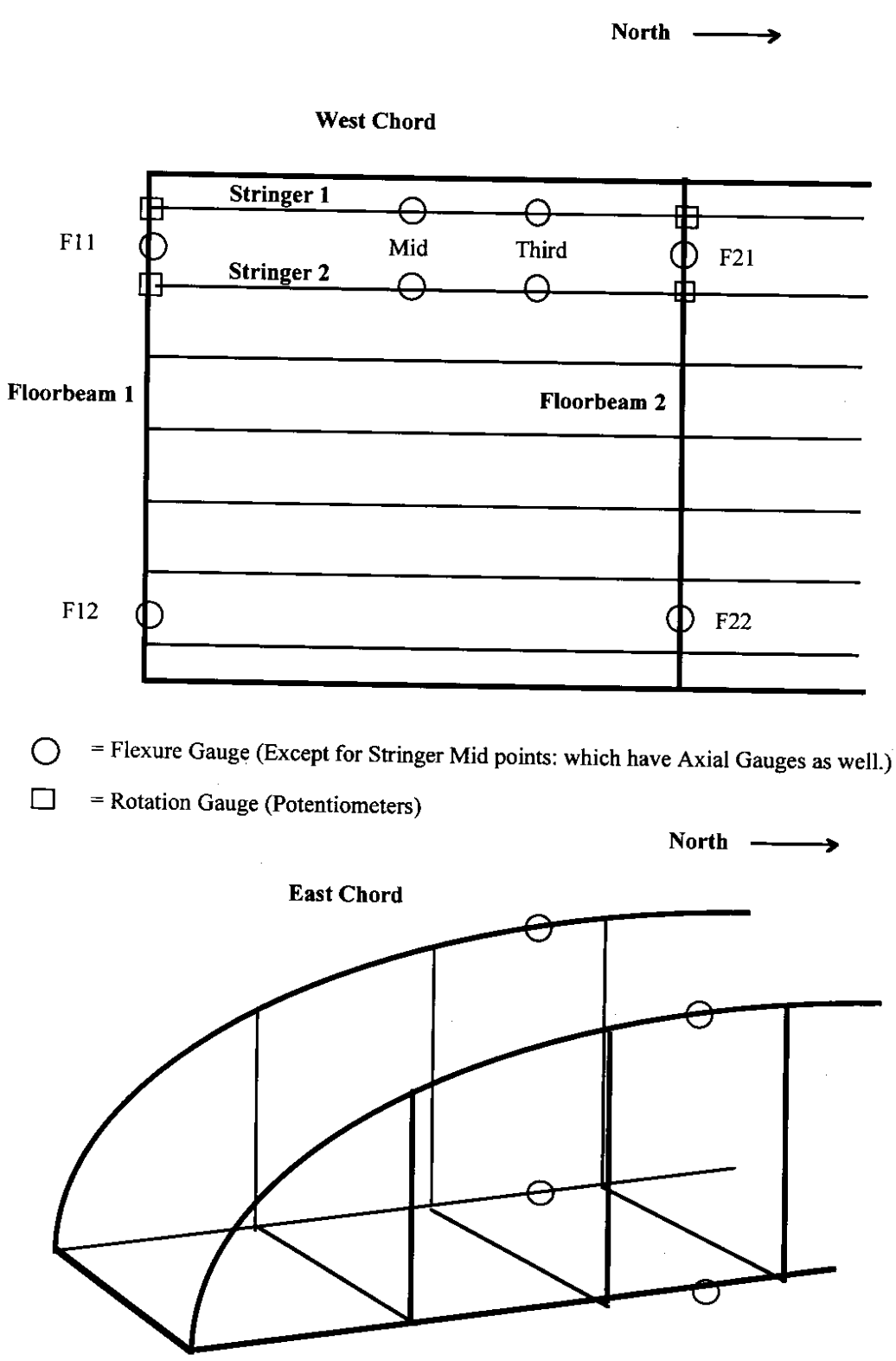

Figure 21. Location and Type of Gauges on the Toutle River Bridge

of the two stringers that measured curvature because these data were useful in establishing neutral axis locations. Rotation gauges were also placed at the ends of these stringers to measure stringer end rotation relative to the floorbeams. The curvature, axial force and rotation measurements of the floorbeams and stringers were used to determine the amount of composite action and end restraint of these members. Strain gages, to measure curvature, were placed on the bottom chord and arch of the west side of the bridge at approximately 1/4 of the bridge length from the south end. In addition, two accelerometers were placed on the bottom chord at the position of the predicted maximum displacement, which was approximately 1/4 of the bridge length from each end. Potentiometers were used to measure the slip of the deck slab relative to the end of the abutment floorbeam in a direction parallel to the floorbeam and the slip of the deck slab relative to a stringer in a direction parallel to the stringer. They were also used to measure the displacement between the end of the bridge and the abutment.

The locations of the strain gauges and potentiometers placed on the Lewis River bridge are shown in Figure 22. Strain gauges were used to measure curvature on the second and third stringers from the west side of the bridge in the north bay. Measurements were taken at mid-span and at a distance of 2/3 of the stringer length from the north abutment. Curvature was also measured on the first floorbeam south of the north abutment between the two instrumented stringers and at the floorbeam mid-span. On the abutment floorbeam, curvature was measured between the two instrumented stringers at the west side of the bridge and at a similar location from the east side of the bridge, as shown in Figure 22. Axial strain was measured by strain gages at mid-span of the two instrumented stringers to establish the neutral axis location. Rotation gauges were also placed at the ends of these stringers to measure their end rotation relative to the floorbeams. To understand the overall bridge performance, strain gages were placed on the west truss of the bridge. They were placed on the end diagonal to measure axial

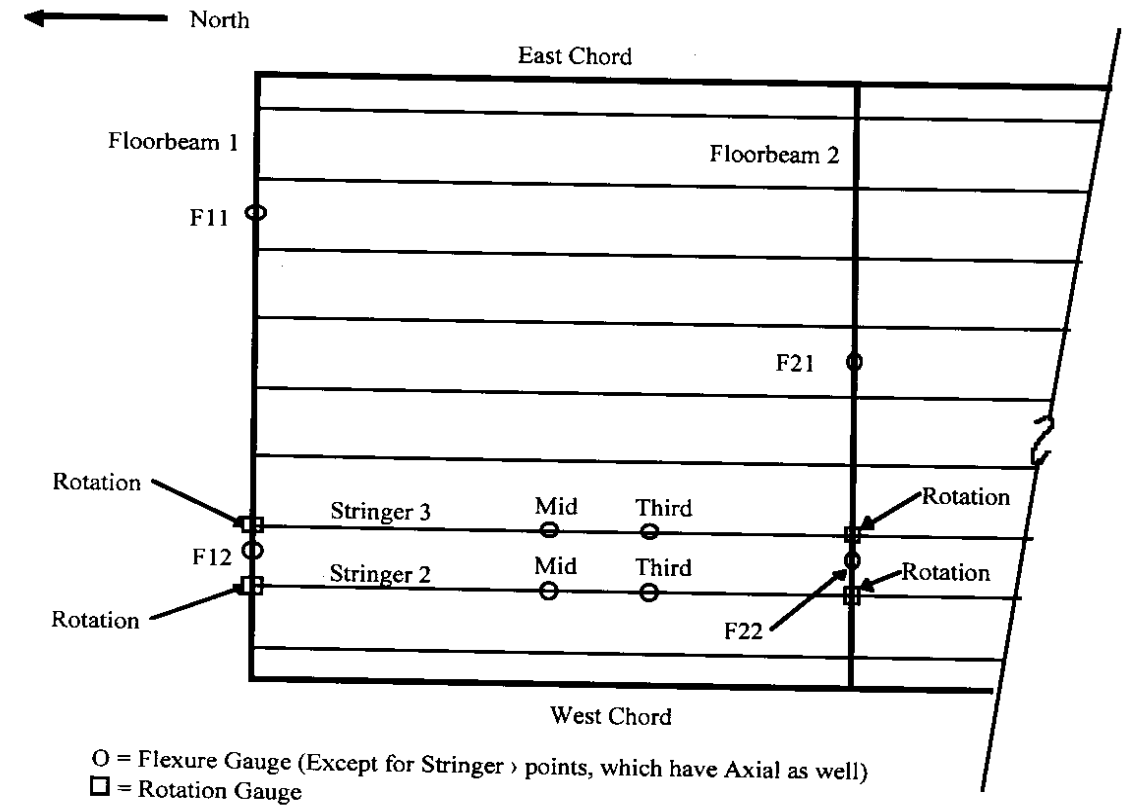

(a) Gauge Locations in Floor - Looking Down, First Span

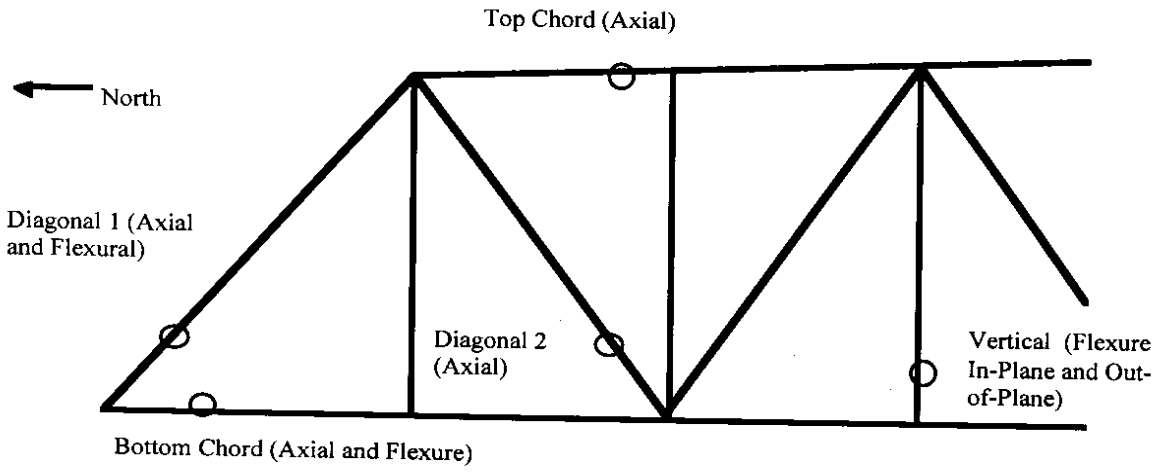

(b) Gauge Locations in West Truss, Looking East

Figure 22. Location and Type of Gauges on the Lewis River Bridge

strain and in-plane curvature, on the top chord of the second bay (from the north) to measure axial strain, on the bottom chord in the first bay to measure axial strain and in-plane curvature, on the diagonal of the second bay to measure axial strain, and on the third vertical hanger from the north to measure both in-plane and out-of-plane curvature. Potentiometers were used to measure the relative slip of the deck slab relative to the end of the abutment floorbeam and in a direction parallel to the floorbeam and the slip of the deck slab relative to a stringer in a direction parallel to the stringer. They were also used to measure displacement between the end of the bridge and the abutment.

CONTROLLED TESTS ON BRIDGES

Controlled tests were performed in early August 1996, immediately after the instrumentation had been installed. In these tests, the bridge was subjected to trucks of known weight and speed that were travelling in known lanes. Two types of controlled testing were carried out. *WSDOT Truck Testing*, involved sending WSDOT trucks of known weight over the bridges under controlled conditions. *Weigh Station Testing* involved recording data from trucks in the normal traffic as they traveled over the bridges. The weights and axle spacing of the trucks were determined later at a nearby official state weigh station. The WSDOT Truck Testing was carried out to determine the following:

- free vibration response of the bridge
- dynamic response amplification or attenuation due to different truck speeds
- effect of braking on bridge response
- effect of loading lane on bridge response
- bridge response due to a truck of given weight and geometry
- amount of floor member composite action and end restraint
- channels that produced a strong and reliable signal, with little drift for uncontrolled testing.

The Weigh Station Testing was carried out to provide supplemental data on bridge response due to different truck weight and geometry, as well as to provide a calibration of the bridge response as a function of truck size so that this information could be used in the uncontrolled testing.

WSDOT TRUCK TESTING

In the *WSDOT Truck Testing*, three trucks were prepared at the WSDOT Vancouver yard. They are referred to as Truck A, Truck B, and Truck C. Truck A was a 9.1m dump truck loaded with concrete barriers. Truck B was a water truck, and Truck C was also a 9.1m dump truck. Gross mass and positions of the axle centerlines are given in Figure 23.

Testing on the Toutle River Bridge was carried out between 1 a.m. and 4 a.m. on the morning of August 13, 1996 and testing on the Lewis River Bridge was carried out between 12 midnight and 4 a.m. on the morning of August 16, 1996. These times were chosen because the southbound lanes I-5 had to be closed for about 7 minutes during each pass while the WSDOT trucks traveled over the bridge. This required co-ordination with WSDOT personnel and Washington State Patrol. Traffic that backed up on I-5 was able to continue over the bridges after each pass while the WSDOT trucks returned to the starting point. Federal Highway Administration (FHWA) researchers independently recorded truck data during the tests on the Toutle River Bridge with wireless instrumentation. The FHWA test data are not reported here since those data are not available.

Truck departures were staged so that the trucks would arrive at the bridge at approximately 30-second intervals. As the trucks approached the bridge, the data acquisition program trigger was activated to record bridge response during loading and for some time after the trucks had left the bridge. Descriptions of each pass for the Toutle River Bridge and the Lewis River Bridge are given in Tables 1 and 2, respectively. During the first three passes, trucks were sent across the bridge one at a time in the right hand lane, since this is the lane that contains the most heavy traffic during normal conditions. Further, most of the instrumentation was set up under this lane. Different target speeds, 113km/h (31.3m/s), 64km/h (17.8m/s) and 16km/h

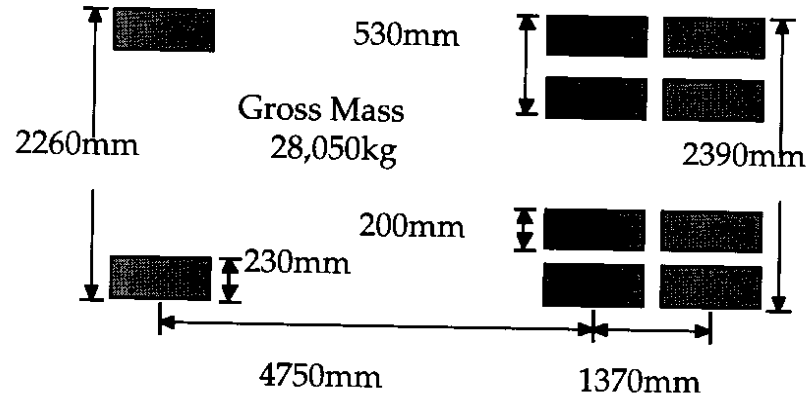

Truck *A*

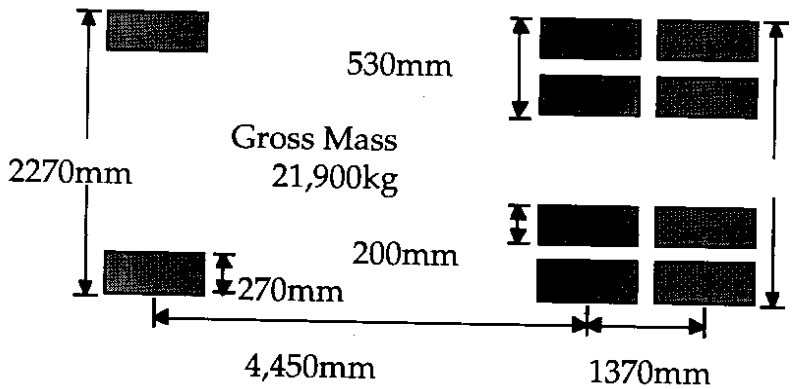

Truck *B*

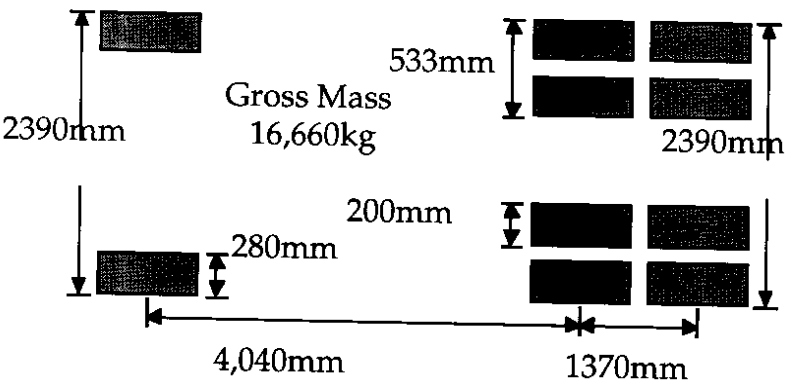

Truck *C*

Figure 23. WSDOT Truck Axle Spacings and Masses

Table 1. Pass Description for Toutle River Bridge

Pass No.	Specified Lane	Target Speed	Truck	Actual Speed
1	Right	31.3m/s (113km/h)	A	24.5m/s (89km/h)
			B	28.6m/s (103km/h)
			C	31.3m/s (113km/h)
2	Right	17.8m/s (64km/h)	A	17.8m/s (64km/h)
			B	17.8m/s (64km/h)
			C	17.8m/s (64km/h)
3	Right	4.47m/s (16km/h)	A	4.47m/s (16km/h)
			B	4.47m/s (16km/h)
			C	4.47m/s (16km/h)
4	Right	(Braking) 31.3 to 0m/s (113 to 0km/h)	A	24.5 - 0m/s (89km/h - 0km/h)
			B	29.0 - 0m/s (105km/h - 0km/h)
			C	31.3-0m/s (113km/h - 0km/h)
5	Center	31.3m/s (113km/h)	A	25.5m/s (92km/h)
			B	28.6m/s (103km/h)
			C	30.8m/s (111km/h)
6	Center	4.47m/s (16km/h)	A	4.47m/s (16km/h)
			B	4.47m/s (16km/h)
			C	4.47m/s (16km/h)
7	Right - Truck A Center - Truck B	31.3m/s (113km/h) 31.3m/s (113km/h)	A	24.1m/s (87km/h)
			B	24.5m/s (89km/h)
8	Right - Truck A Center - Truck B	4.47m/s (16km/h) 4.47m/s (16km/h)	A	4.47m/s (16km/h)
			B	4.47m/s (16km/h)

Table 2. Pass Description for Lewis River Bridge

Pass No.	Specified Lane	Target Speed	Truck	Actual Speed
1	Right	31.3m/s (113km/h)	A	26.8m/s (97km/h)
			B	28.6m/s (109km/h)
			C	31.3m/s (113km/h)
2	Right	17.8m/s (64km/h)	A	17.8m/s (64km/h)
			B	17.8m/s (64km/h)
			C	17.8m/s (64km/h)
3	Right	4.47m/s (16km/h)	A	4.47m/s (16km/h)
			B	4.47m/s (16km/h)
			C	4.9 m/s (18km/h)
4	Right	(Braking) 31.3 to 0m/s (113 to 0km/h)	A	26.8-4.47m/s (97km/h - 16km/h)
			B	29-0m/s (105km/h - 0km/h)
			C	30.8-0m/s (111km/h - 0km/h)
5	Center	31.3m/s (113km/h)	A	26.8 m/s (97km/h)
			B	29.1m/s (47km/h)
			C	30.8m/s (111km/h)
6	Center	4.47m/s (16km/h)	A	4.47m/s (16km/h)
			B	4.47m/s (16km/h)
			C	4.47m/s (16km/h)
7	Right - Truck A	31.3m/s (113km/h)	A	24.1m/s (87km/h)
	Center - Truck B	31.3m/s (113km/h)	B	24.5m/s (89km/h)
	Left - Truck C	31.3m/s (113km/h)	C	24.5m/s (89km/h)
8	Right - Truck A	4.47m/s (16km/h)	A	4.47m/s (16km/h)
	Center - Truck B	4.47m/s (16km/h)	B	5.4 m/s (19km/h)
	Left - Truck C	4.47m/s (16km/h)	C	6.3 m/s (23km/h)
9	Left - Truck A	4.47m/s (16km/h)	A	3.1 m/s (11km/h)
	Center - Truck B	4.47m/s (16km/h)	B	4.47m/s (16km/h)
	Right - Truck C	4.47m/s (16km/h)	C	4.9 m/s (18km/h)
10	Left	4.47m/s (16km/h)	A	4.47m/s (16km/h)
			B	4.47m/s (16km/h)
			C	4.47m/s (16km/h)

(4.47m/s), were used in separate passes so that dynamic amplification effects could be measured. Sometimes the trucks were not able to achieve these speeds. During Pass 4 the trucks were required to brake from 113km/h (31.3m/s) to almost a complete stop on the bridges. Passes 5 and 6 were carried out at target speeds of 113km/h (31.3m/s) and 16km/h (4.47m/s) in the center lane. Passes 7 and 8 were carried out with several trucks travelling over the bridge together at the same speed. Pass 8 on the Lewis River bridge was redone as Pass 9 because of problems in the initial recording. On the Lewis River Bridge a final pass was carried out in the left-hand lane. This left lane loading was not carried out over the Toutle River Bridge because the left-hand lane of the Toutle River Bridge was closed for construction.

FREE VIBRATION RESPONSE

Free vibration response was obtained after the trucks had crossed the bridge at a speed of 113km/h (31.3m/s). To clearly identify the response frequencies, a Fourier transform was carried out on the free-vibration response with the fast-Fourier technique. Following standard methods, damping was estimated from the decay in response after several cycles of loading according to (Clough and Penzien 1994).

The fundamental period of vibration observed in the west chord and arch of the Toutle River Bridge was 1.11s. This agrees well with the analytical prediction of 1.08s. While the associated mode shape, which approximated a full sine-wave over the length of the bridge, had a small mass participation of 0.88 percent in the vertical direction, the mode may have been excited strongly by trucks that traveled across the bridge. The deformed shape of the arch bridge under the local truck load was observable with the eye. The average computed damping was 0.5 percent. The result was a slow decay of response, as shown in Figure 24. Response periods of 0.53s and 0.33s were also measured from the frequency domain analysis of the measured response.

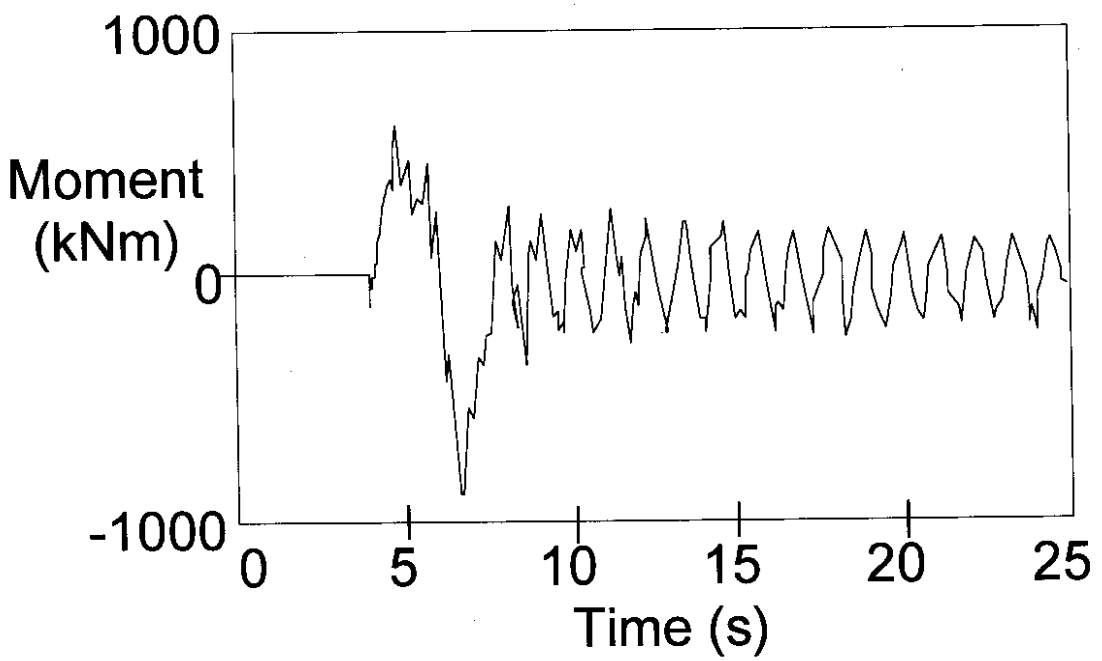

Figure 24. Toutle River Bridge West Chord Moment vs. Time, Truck A, Pass 1

Floorbeams had measured response periods of 1.11s, 0.5s, 0.4s, 0.33s, 0.21s, 0.15s, and 0.09s. The theoretical response period of the floorbeam was 0.09s, assuming computed end fixities and no composite action. Several of these frequencies were similar to the overall bridge response, indicating that bridge response affected the floor system behavior.

The computed stringer frequency of 0.053s could not be detected clearly. Global bridge modes of vibration controlled the response. Some difference in the contribution of modes was observed with the different trucks. This may have been a result of the difference in suspension characteristics of the trucks or the added mass of the vehicle.

In the Lewis River bridge, a measured fundamental response period of 0.5s was seen in the data obtained for all members. This is close to the theoretical computed fundamental period of vibration of 0.48s.

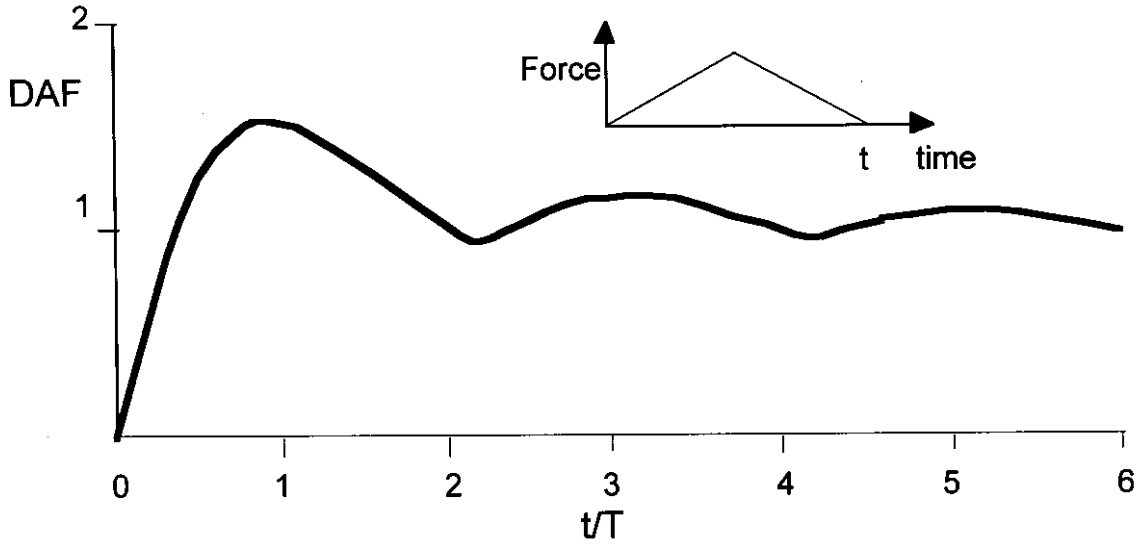

Figure 25. Dynamic Amplification Factor Due to Triangular Load

FORCED VIBRATION TESTS

Amplification or attenuation of dynamic response was determined from the experimental results, and this was correlated to theoretical predictions. The theoretical predictions were largely based on the theoretical dynamic amplification factor, DAF, obtained from the triangular pulse loading, as shown in Figure 25. This triangular time-dependent variation in loading closely simulates the dynamic loading on floorbeams and stringers, but it is a relatively poor approximation of the dynamic loading and resulting response for the truss and tied arch system. Figure 25 shows that amplification of dynamic response is expected when $0.4 < t/T < 2.0$, and attenuation is expected when $t/T < 0.4$. A change in dynamic response of no more than 16 percent would be expected for $t/T > 2.0$.

During the controlled testing, truck passes made at 16km/h were considered to be "static" loading because they were too slow to cause dynamic effects. This is verified in Figure 25, which shows that the t/T ratio exceeds 20 for the floorbeams and stringers with this truck speed. Therefore, the experimentally determined dynamic amplification was

determined by dividing the maximum response by the maximum dynamic response for the same vehicle loading at the 16km/h truck velocity.

The measured DAF varied between 0.9 and 1.7 for the floorbeams of the Toutle River bridge. Larger amplifications were noted for the more lightly strained portions of the girder and for the lighter vehicles travelling at higher speeds. The measured DAF for stringers under the right lane was between 0.6 and 1.1. Lighter vehicles caused slight amplification or small attenuation, whereas heavier trucks produced significant attenuation of response. The t/T ratios for the floorbeams and stringers of the Toutle River bridge varied between 5.1 and 10.4, and so theoretical predictions would suggest very little attenuation or amplification of the DAF ratio. Very light or indirect loading of members resulted in greater variation in dynamic response, but this is not a critical issue because the static response is small under these conditions, and the degree of amplification is not particularly relevant.

The chord and arch response of the Toutle River bridge resulted in DAF ratios of between 0.94 and 1.35. The larger ratios occurred in the more lightly loaded elements. Virtually no amplification was noted in heavily loaded members at the 64km/h truck speed. Heavily loaded members had amplifications of 5 percent to 15 percent (DAF values of between 1.05 and 1.15) with the high speed (113km/h) vehicles.

The measured DAF varied between 0.8 and 1.2 for the floorbeams of the Lewis River bridge. The larger amplifications were usually noted for the 64km/h vehicle speed. The stringers of the Toutle River bridge exhibited DAF values that varied between 0.6 and 1.2. Note that the computed t/T ratios for the floorbeam and stringers of the Toutle River bridge varied between 3.2 and 12.4 for the dynamic tests, and therefore, Figure 25 suggests that little or no amplification was expected. The variation in these experimental values was larger than may have been expected, but greater amplification and attenuation is possible if the spring stiffness of the truck suspension systems is considered in the

analysis. Under these conditions the vibration is a two-degree-of-freedom system, and the dynamic amplification is inherently more complex.

Several passes of truck traffic on both bridges required emergency braking on the bridges. The maximum response of the bridge elements was then compared to the maximum values noted with constant vehicle speed. The results of these measurements indicated that the braking forces caused no significant effect on any of the members considered in this study for either bridge.

END RESTRAINT AND COMPOSITE ACTION OF FLOORBEAMS

Knowledge of the degree of composite action and end restraint allows engineers to estimate the stresses along the beam length and to approximate the end connections. This information is needed to establish the stress range at critical locations in the structure and to evaluate the fatigue life.

The floorbeam end spring flexibility ratio was defined as $EI/(Lk_r)$, where E is Young's modulus for steel, L is the length of the floorbeam, and k_r is the member end rotational stiffness, with units of moment/rotation shown in Figure 17 and obtained as described earlier. I is the second moment of area of the section calculated with an average weighted approach, since I actually varied along the length of the section as shown in Figure 26. This flexibility ratio, $EI/(Lk_r)$, is infinite for a pinned end condition and is zero for a fully restrained condition. The connections between the floorbeams and

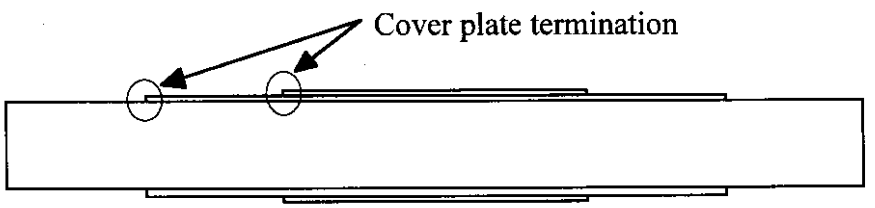

Figure 26. Elevation of Interior Floorbeam of Lewis River Bridge

chords in both bridges were assumed to be fully restrained because of the connection details but the flexibility of the members connecting to the floorbeams was relatively large. Values of computed $EI/(Lk_r)$ were 7.1 and 1.1 for the interior of the Lewis River and Toutle River bridges respectively.

The smaller flexibility (and higher rotational stiffness) of the Toutle River bridge floorbeam end connections implied greater moments at the end connections of the Toutle River floorbeams than for the Lewis River bridge floorbeams. However, the Lewis River bridge was subject to larger moments along the length of the beam where riveted end-plates terminate.

No shear studs were placed on the top flange of the floorbeams. However, composite action may have existed because of bond on the surface of the beam. The amount of composite action in the floorbeams was assessed by comparing moments based on measured curvatures to those predicted from moment diagrams. The moment diagrams were developed by assuming different degrees of end restraint and the applied load distribution. The moments based on measured curvature were computed by multiplying the curvature measured at points along the length of the floorbeam by the composite flexural stiffness $(EI)_{comp}$, as well as by non-composite flexural stiffness $(EI)_{non\text{-}composite}$. These moments were plotted on the bending moment diagram. The degree of composite action at any point along the length of a floorbeam may be established by comparing moment based on member curvature and that computed for the member end restraint.

Figure 27 shows bending moment diagrams along the length of an interior floorbeam on the Lewis River bridge (Truck A travelling at 16km/hr in Pass 3). Rotational end restraint assumptions for the three bending moment lines were full restraint (FR), pinned end restraint, and partial restraint (PR). The partial end restraint

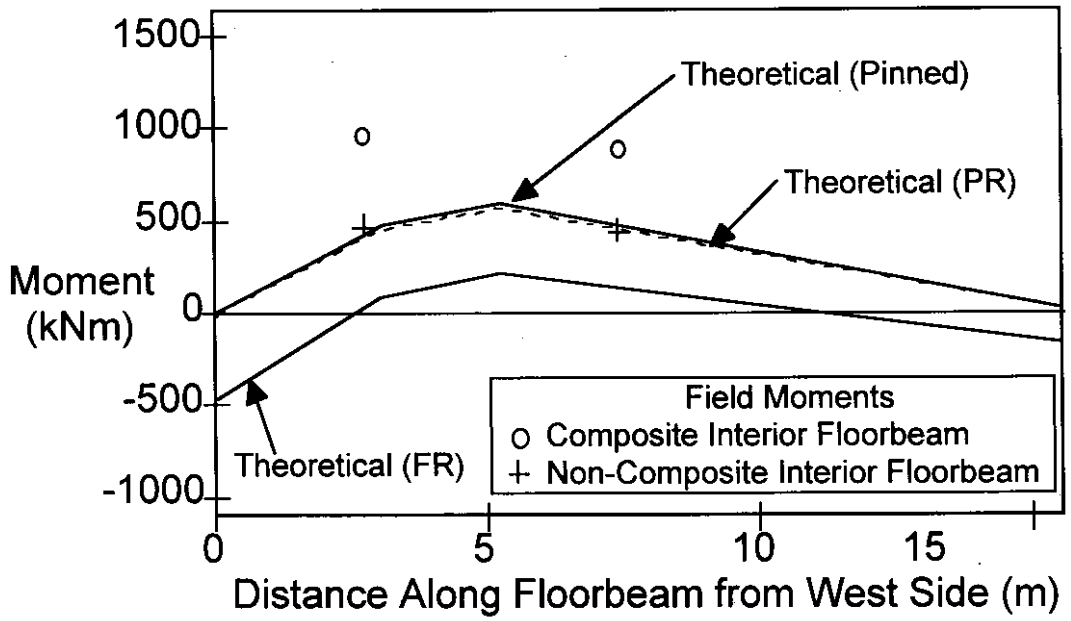

Figure 27. Lewis River bridge Interior
Floorbeam Bending Moment, Truck A, Pass 3

was developed with the spring stiffness k_r shown in Figure 17. For the pinned case the moment at each end of the beam was zero. The partially restrained moment diagram was very close to the pinned end condition for the interior floorbeams of both bridges.

Figure 27 shows the bending moment at the floorbeam gauge locations for an interior floorbeam on the Lewis River bridge. It was computed from the measured curvature, which assumed both fully composite and non-composite conditions. Fully composite action assumed an effective width of floor slab equal to 25 percent of the span length (AISC-LRFD 1994). The non-composite bending moments closely coincided with the bending moment diagrams for little or no end restraint. The conclusion was that very little composite action was present in the interior floorbeams of either bridge. This analytical result was confirmed by visual inspection of the concrete deck, which revealed significant cracks above the floorbeams.

The apparent composite action and end restraint of the abutment floorbeams of the Lewis River bridge were much larger. The larger end restraint was caused by the stiff

bottom chord and end diagonal of the truss, which framed into the abutment floorbeam connection. The apparent composite action in the abutment floorbeam was not believed to be caused by composite action but by the large bending stiffness induced by the steel framing that supported the finger joint at the top of the abutment floorbeam.

END RESTRAINT AND COMPOSITE ACTION OF STRINGERS

The degree of composite action and the end restraint of stringers were equally important in the fatigue evaluation. Whereas the Lewis River bridge contained no shear studs between the concrete deck and the stringers, the Toutle River bridge had shear connectors over the length of each stringer. Stringers had both axial and curvature gages at the same position along their length. Therefore, the position of the neutral axis, y_{na}, from the bottom of the lower flange could be computed. At the ends, rotation was measured with respect to the floorbeams, and this could be used indirectly in the evaluation of end restraint.

The degree of composite action, *CA*, was defined as

$$CA\ (\%) = \frac{y_{na} - y_s}{y_c - y_s} \times 100(\%) \qquad \text{(Equation 2)}$$

where y_{na} is the experimental neutral axis measured from the bottom of the section, y_c is the neutral axis position of the fully composite section measured from the bottom of the section, and y_s is the neutral axis of the bare steel beam or one-half of the depth of the steel section. Full composite action assumed an effective floor slab width equal to the minimum spacing of the stringers (AISC-LRFD 1994). The effective second moment of area, I_{eff}, could be closely estimated from the composite second moment of area, I_c, and the bare steel second moment of area, I_s, (Crocker 1997) using the equation

$$I_{eff} = I_s + (I_c - I_s)\ \frac{CA\ (\%)}{100\ (\%)} \qquad \text{(Equation 3)}$$

Figures 28 and 29 show the measured neutral axis section at peak curvature during each of the passes of Truck A for the Lewis River Bridge and the Toutle River bridges, respectively. The composite action computed by Equation 1 from the measured neutral axis locations may be regarded as an upper bound because it was measured at the mid-span of the stringers. During left or center lane passes, the instrumented stringers were subjected to very small bending moments in comparison to right lane passes. Neutral axis (N.A) positions computed from the left or center lane passes were therefore less reliable. However, left or center lane passes did show higher N.A. positions than did the right hand lane passes indicating that the degree of composite action decreased with greater loading.

The amount of composite action ranged from 40 to 60 percent in Stringer 3 and 80 to 100 percent in Stringer 2 on the Lewis River bridge, as shown in Figure 28. Stringer 3 was directly beneath the right-hand lane, and Stringer 2 was nearer the side of the bridge, as shown in Figure 22.

In the Toutle River Bridge, the amount of composite action ranged from 40 to 50 percent in Stringer 2 and 70 to 80 percent in Stringer 1, as shown in Figure 29. Stringer 2 was directly beneath the right-hand lane and Stringer 1 was nearer the side of the bridge. The stringer that carried the majority of the traffic loading showed less composite action in both cases. This suggests that composite action that developed as a result of friction and natural bond between the steel and concrete had been partially lost under repeated heavy loading.

The position of the stringer moment and neutral axis for the Toutle River Bridge is shown against time for Truck A, Pass 3, in Figure 30. This shows that the position of the neutral axis did not change significantly when the truck was on the bridge. The Lewis River Bridge showed more variation.

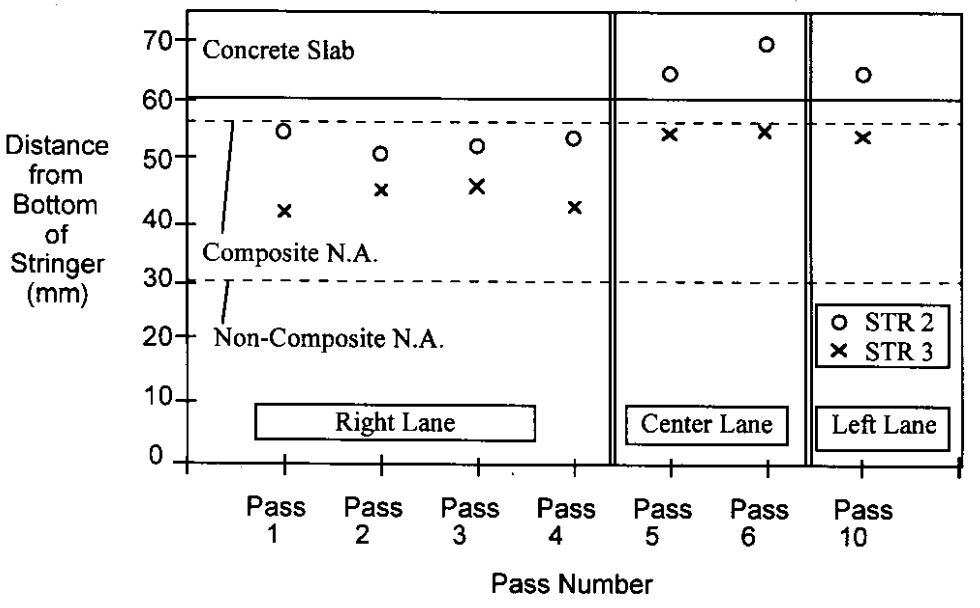

Figure 28. Stringer Neutral Axis Position, Truck A, Lewis River Bridge

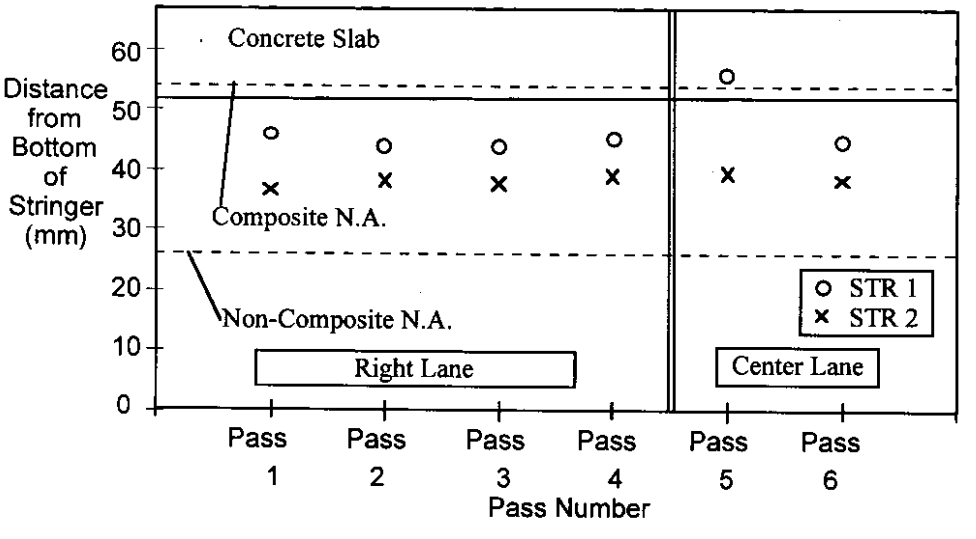

Figure 29. Stringer Neutral Axis Position, Truck A, Toutle River Bridge

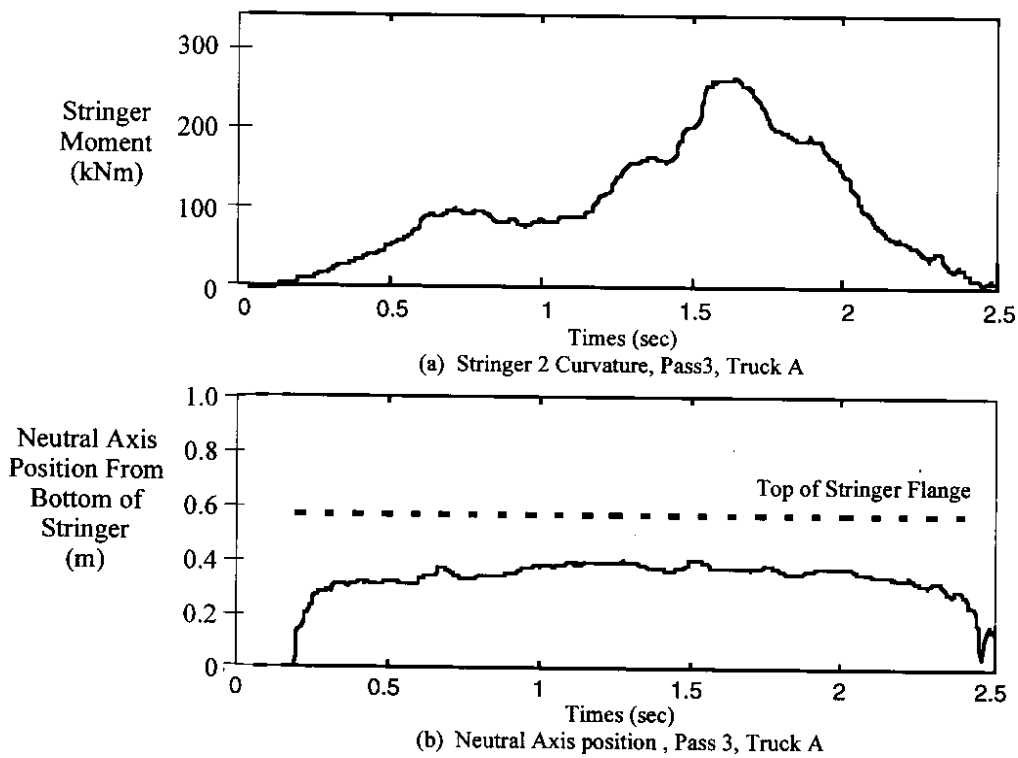

Figure 30. Moment and Neutral Axis Position
for Stringer on Toutle River Bridge Due to Truck A Pass

The rotation at the ends of the stringers with respect to the floorbeams was measured with rotation measuring devices. However, rotation did not provide a direct measure of member rotational end restraint. The relative rotation, θ, measured at each end of the floorbeam was a combination of the rotation due to stringer curvature, θ_{str}, rotation due to floorbeam twisting, $\theta_{fb\text{-}twist}$, and rotation from floorbeam differential vertical displacement, $\theta_{vertical}$, as shown in Figure 31 (Arima 1997).

The components of rotation due to the stringer curvature alone, θ_{str}, were obtained by decomposing the rotation into components as shown. Details of this procedure are described elsewhere (Crocker 1997). The rotational spring stiffness, k_r, required to develop this rotation under the known truck loadings was computed. This stiffness, k_r, is written in terms of the dimensionless end restraint flexibility ratio, $EI/(Lk_r)$, (see Table 3).

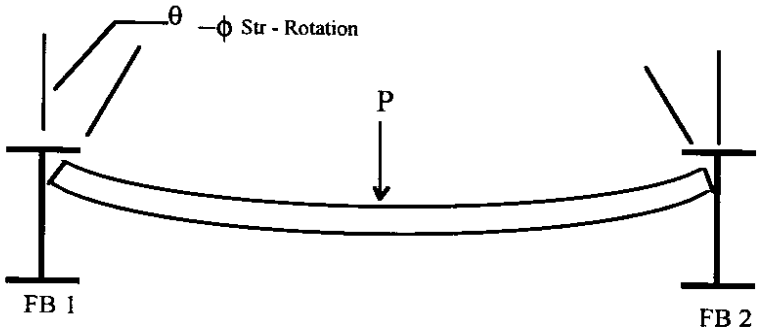

(a) Rotation due to stringer curvature force P.

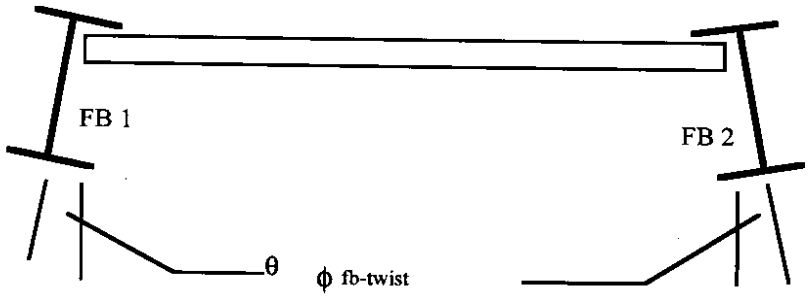

(b) Rotation due to the Floorbeam twisting which is caused by the stringer curvature.

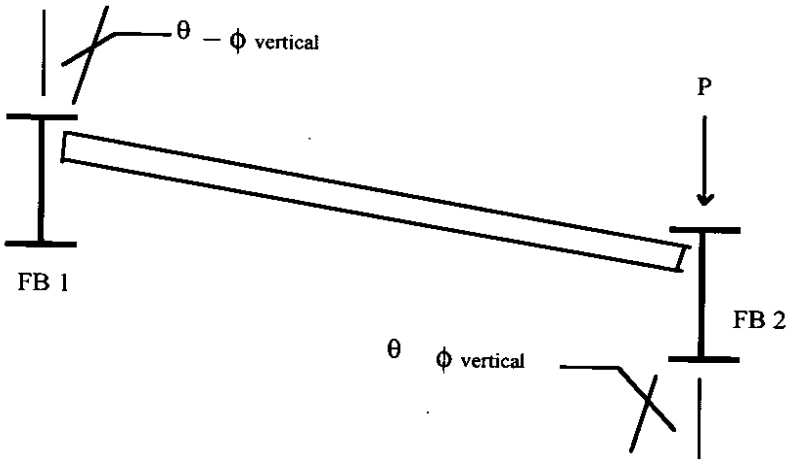

(c) Rotation due to the floorbeam vertical-differential-displacement.

Figure 31. Measured Rotation

Table 3. Stringer Rotational Spring Flexibility Ratios, $EI/(Lk_r)$

Lewis River Bridge	Abutment End	infinite
	Interior End	0.49
Toutle River Bridge	Abutment End	7.0
	Interior End	1.4

The ends of the stringers at the abutment floorbeams, where stringers framed into only one side of the beam, had higher flexibility than at the interior floorbeams. Higher end flexibility, $EI/(Lk_r)$, resulted in a lower moment at the connection of the stringer to the floorbeam. The stringer end moment produced tension at the top of the stringer at the critical cope, which was the source of cracking. Internal ends of stringers in the Lewis River Bridge were therefore more likely to sustain fracture than those in the Toutle River Bridge.

The lengths of the stringers in both bridges were similar; the stringer section modulus was approximately 40 percent greater for the Lewis River bridge, and the spacing of the stringers in the Toutle River Bridge was 1.30 times that of those in the Lewis River Bridge. Significantly larger moments were expected at the midspan of the stringers of the Toutle River Bridge than those of the Lewis River Bridge.

BRIDGE DEFLECTIONS DURING CONTROLLED TESTING

Accelerometer readings were only taken on the Toutle River Bridge. Accelerations were integrated twice to get time-dependent displacements. Accelerations in the slower passes were too small to provide reasonable deflection results. The displacements obtained at one-quarter of the bridge length from the abutment showed considerable drift, as shown in Figure 32 (Crocker 1997). After drift was corrected for, the vertical displacement range was computed as 33mm for Truck A in Pass 1 and 41mm for Trucks A and B together in Pass 7.

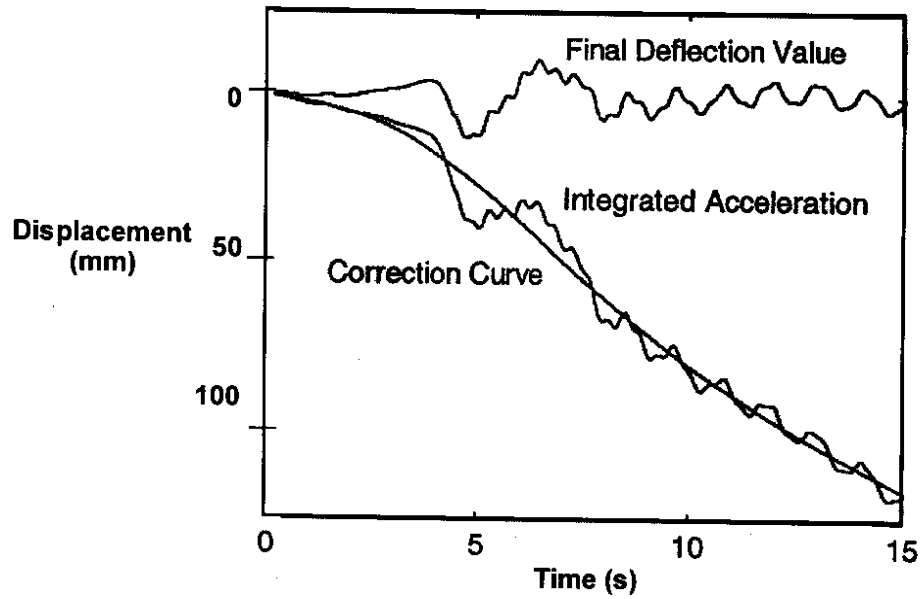

Figure 32. Displacement, based on Acceleration Integration, Versus Time

WEIGH STATION TESTING

Weigh station testing was carried out during the day on September 4 on both bridges. Trucks that appeared to be heavily loaded and that had easily distinguishing features were identified at the Toutle River bridge. The response of these trucks was recorded and specifically identified. After the truck had crossed the bridge, a description of the truck was sent to the Washington State Patrol weigh station located approximately 8km south of Toutle River bridge. When the truck arrived at the weigh station, the axle weights and axle dimensions were recorded. The truck driver was asked whether the truck would continue south over the Lewis River bridge, and descriptions of trucks continuing beyond the Lewis River bridge were phoned to the bridge site. Researchers at the Lewis site attempted to identify the trucks as they crossed. The bridge response was recorded and identified for further identification. Only some of the trucks sent were positively identified at the Lewis River Bridge. For other trucks good data were difficult to obtain because of heavy simultaneous traffic.

The member responses obtained from the weigh station testing were related to the truck loading. Stringer flexural response was controlled by maximum axle weight, since truck axle spacings were generally long enough that load from only one axle was carried by a stringer at any time. Maximum axle weight versus stress range for the Toutle River Bridge stringers was plotted for the Weigh Station test trucks (Figure 33) (Crocker 1997). The total weight of three WSDOT trucks with a target speed of 113km/h are also plotted in Figure 33. Both axles were considered to be acting on the stringers simultaneously because the axle spacing was close in comparison to the longer trucks. Lower stresses resulted from WSDOT trucks of a given weight because the distance between axles caused a lower stress than that due to a point load of the same total weight. The scatter of the resused for all trucks resulted from different axle spacings and suspension systems in the trucks.

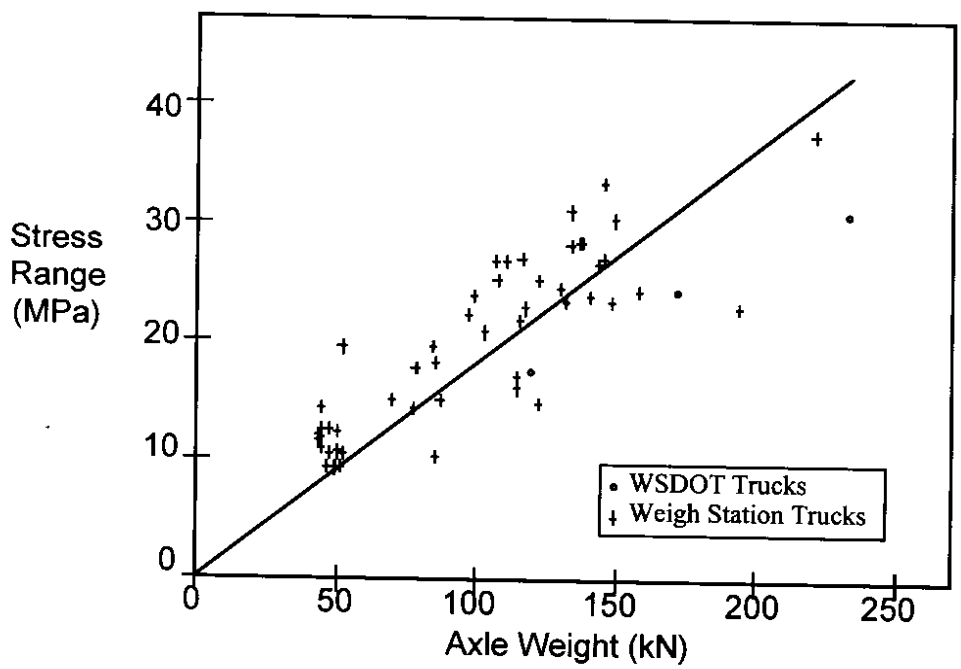

Figure 33. Stringer Stress Range versus Axle Weight
(Toutle River Bridge)

Floorbeam and chord response were correlated to total truck weight, since simultaneous loading from all axles of a truck affected these members. Stress range is plotted against weight for the weigh station trucks and the WSDOT trucks on the Toutle River Bridge in Figures 34 and 35. Stresses caused by the WSDOT trucks were greater than the other trucks because the axles were closer together, causing more of a point loading on the members. The scatter of the results for all trucks resulted from different axle spacings and suspension systems in the trucks.

Linear curve fits were used to obtain a relationship between stress range magnitude and truck or axle weight. This allowed truck weight to be estimated from the stress ranges. Uncontrolled truck testing used these curves to estimate the magnitude and number of cycles of repetitive loading on members of the bridge for the fatigue life calculation.

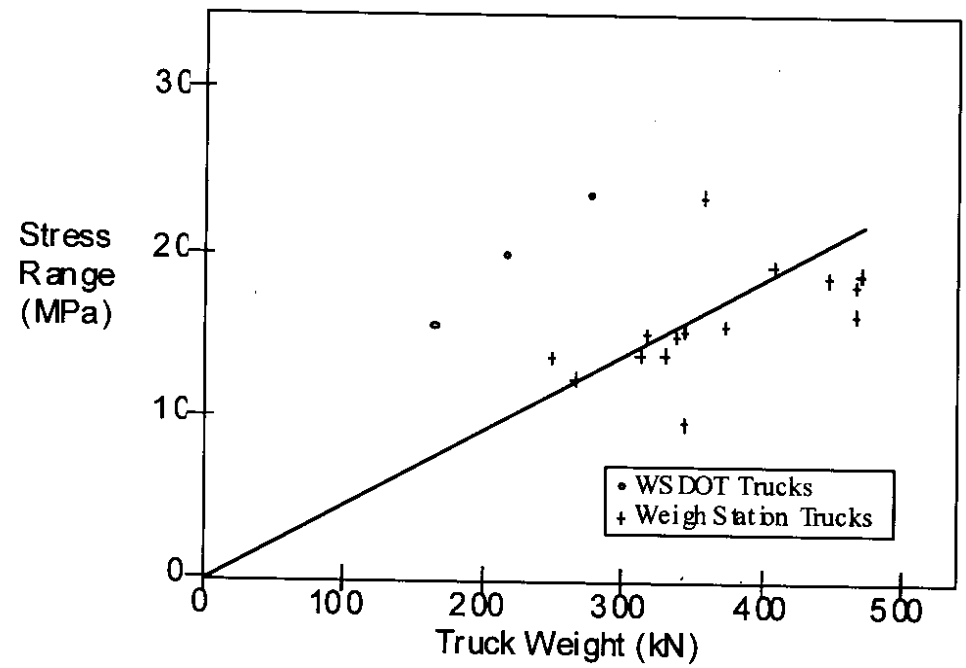

Figure 34. Floorbeam Flexural Stress Range versus Truck Weight (Toutle River Bridge)

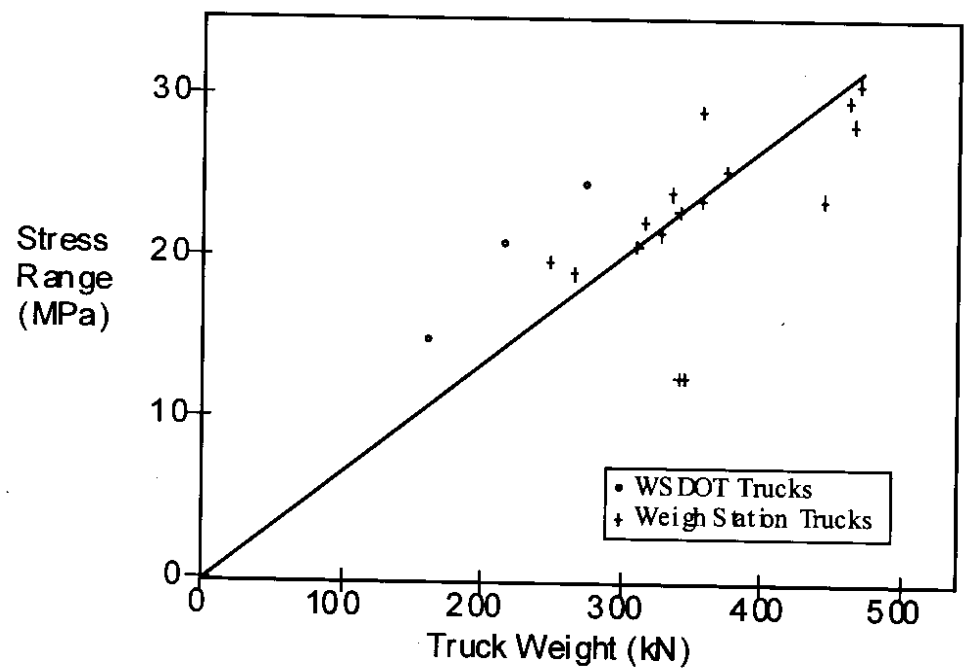

Figure 35. Chord Flexural Stress Range versus Truck Weight (Toutle River Bridge)

UNCONTROLLED TRAFFIC MEASUREMENTS AND FATIGUE LIFE

GENERAL COMMENTS

As noted in earlier chapters, the Toutle River and Lewis River bridges were instrumented, and controlled tests were performed. The controlled tests were used to establish a fundamental understanding of the bridge behavior, and they provided a calibration between bridge response and truck loading. The fatigue concerns of these bridges relate to actual highway truck loading, but the size and frequency of these trucks are unknown. As a result, a major portion of this research study consisted of measuring bridge response under actual truck loading. The results of this information provided indications of the load spectra experienced by these bridges. These spectra could provide insight into the fatigue life of WSDOT's many other riveted steel bridges in the I-5 corridor. However, the measured data were also directly useful in estimating the fatigue life of these two bridges. This chapter provides a summary of these uncontrolled truck traffic measurements, the correlation of these measurements to the truck traffic, and estimation of the fatigue life of critical components in the two bridges. More detailed descriptions of these issues may be obtained elsewhere (Arima 1997, Crocker 1997, and Wong 1997).

UNCONTROLLED FIELD MEASUREMENTS

The instrumentation and data acquisition system used in the controlled load tests were also used to measure uncontrolled truck traffic. The uncontrolled truck measurements started immediately after the controlled tests had been completed and continued for more than three weeks. Continuous monitoring of traffic for that period would have produced a phenomenal quantity of data. As a result, the data acquisition system was modified for uncontrolled tests. The channels were continuously monitored, but only data that were of

interest to the fatigue study were actually recorded. To do this, a triggering mechanism and a recording interval had to be established for both bridges, as noted in earlier discussion.

The triggering was set so that the heaviest trucks would all be recorded, since heavy trucks cause the greatest portion of fatigue damage, but automobiles and light trucks would not be recorded. The goal was to obtain data on all trucks with a gross weight of over 133.5 kN. A number of trucks lighter than 133.5 kN were obviously recorded, and a few trucks approximating this limit but traveling in an unusual lane were missed. However, all trucks significantly larger than this limit, regardless of the lane of travel, were captured in the data. This dramatically reduced the quantity of data and simplified the data analysis process. Critical channels that clearly responded to moderate and heavy trucks but did not respond to lighter vehicles were selected for each bridge as the trigger channels. These critical channels were continuously monitored, and when the monitored signal exceeded the selected threshold, a short window or interval of data was recorded.

The window was about 6 to 10 seconds long. Because exceedance of the threshold indicated that the bridge was well into a significant event, the recording interval was actually started approximately 1 or 2 seconds before the threshold was reached. This delay time was different depending on the bridge.

The data acquisition system operated in this mode throughout the uncontrolled testing. However, the process was interrupted. First, the disk drives in the data acquisition systems stored up to 2 GB of data. As a result, the disk drives occasionally filled to capacity, and data could not be stored until the disk had been downloaded by the researchers. Several hours were required to download data from the computer disk drives to transfer tapes, clear the drives, and restart the data acquisition process. Second, the researchers temporarily intervened as frequently as every 24 hours to adjust the electronic equipment and minimize problems with drift. Finally, drift of the electronic systems resulted in one or two shutdowns, which produced gaps in the recorded truck traffic.

Nevertheless, the computers and data acquisition systems operated without human intervention or observation for long periods.

Despite the interruptions, large quantities of data were recorded. For the Toutle River Bridge, data were recorded for 470.35 hours (19.6 days), excluding interruptions, and 73,968 trucks were identified. This resulted in 3794 trucks recorded for an average 24-hour period. A 1993 traffic count for Kelso estimated that on average, 4,100 tractor trailers passed southbound on I-5 through Kelso. A number of these trucks would be nearly empty, so it appears that the measurement process truly captured the bulk of the truck traffic. For the Lewis River bridge, 360 hours (15 days) of recording time and 10 GB of data were recorded. The number of trucks recorded at the Lewis River bridge was somewhat smaller than the number recorded at the Toutle River bridge. However, the number of heavy trucks was similar for the two bridges.

FREQUENCY AND LOAD SPECTRUM

Prior discussion has noted that the approximate axle weight for vehicles and the approximate gross vehicle weight could be estimated from the dynamic stress ranges recorded during the tests. These calibrations are illustrated in Figures 33, 34, and 35. The results of these calibrations permitted direct development of an average daily load spectrum for the two bridges. Figures 36 and 37 show the estimated total truck load spectra for the Toutle River and Lewis River bridges, respectively. The spectra are represented as histograms for an average 24-hour period. Comparison of these figures provides evidence of validity and compatibility of the measured data. Recall that 133.5 kN was the target measurement threshold for these uncontrolled truck measurements; the histograms are quite comparable for both bridges for trucks larger than this threshold. A significant number of trucks with estimated gross weights of between 133.5 kN and 555 kN were noted each day for both bridges. A local peak can be noted in the spectrums, and the vehicle weight for

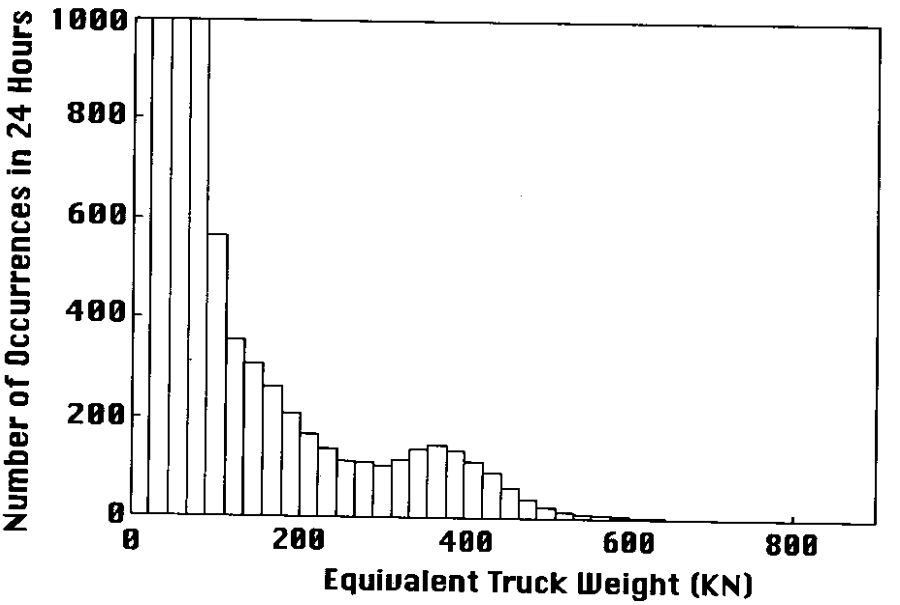

Figure 36. Estimated Total Truck Load Spectrum for Toutle River Bridge

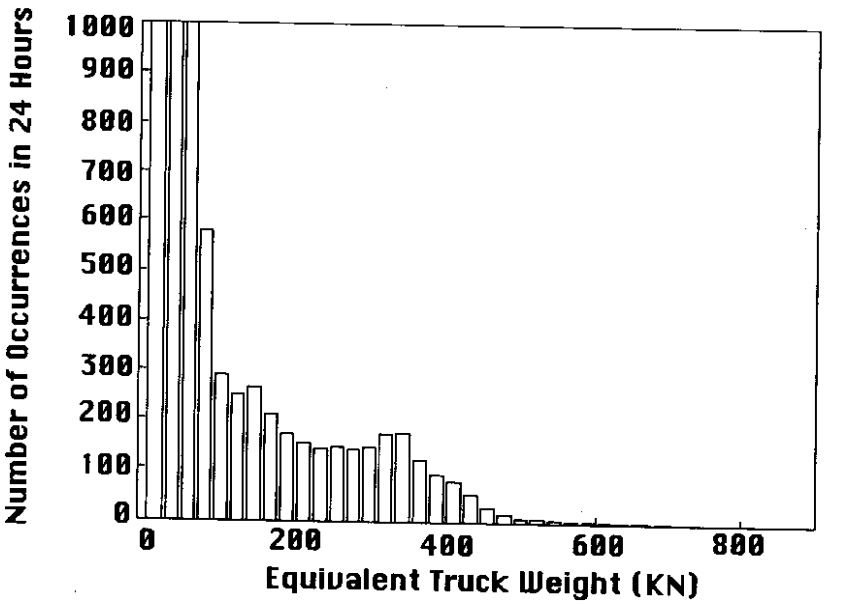

Figure 37. Estimated Total Truck Load Spectrum for Lewis River Bridge

these peaks is approximately 355 kN for the Toutle River bridge and between 335 kN and 355 kN lbs for the Lewis River bridge. A very few trucks with estimated gross weights of greater than 550 kN were noted on both bridges. Note that these estimated vehicle weights are approximate because of the scatter shown in Figures 33, 34, and 35. Furthermore, multiple trucks on the bridge were sometimes identified as a single, heavier truck because they traveled so closely together. Although the spectrum is approximate, the measured data accurately represent the effective stress ranges experienced by these bridge elements.

The stringers of both bridges were dominated by the axle loads of these trucks. Tandem or multiple axles were combined as a single axle. Figures 38 and 39 show the axle load spectrum for the Toutle River and Lewis River bridges, respectively. These spectra are again represented as histograms for an average 24-hour period. The correlation between these is also good but clearly not as good as the estimated total vehicle weight. Both curves illustrate a local peak at approximately 160 kN, but the peak is more rounded and there are fewer very heavy axles for the Toutle River bridge. The scatter in calibration is generally greater for the axle loads because these loads commonly contained double or triple axles, and so these spectra are inherently less accurate. However, the estimated axles fit reasonably well within legal axle and wheel load limits for Washington State, and this provides further evidence that the data considered here were reasonable and relevant for fatigue evaluation. Again, the stress ranges experienced by the stringers of these two bridges were independent of the truck load spectra, and so the fatigue analysis was not controlled by limitations in the accuracy of these load spectra.

These measured data can be used to estimate the fatigue life of critical elements within both bridges. However, truck traffic varies from day to day, month to month, and year to year. This variation must be considered if the fatigue life of these elements is to be reasonably estimated. The day to day variation was considered in the measurements. The

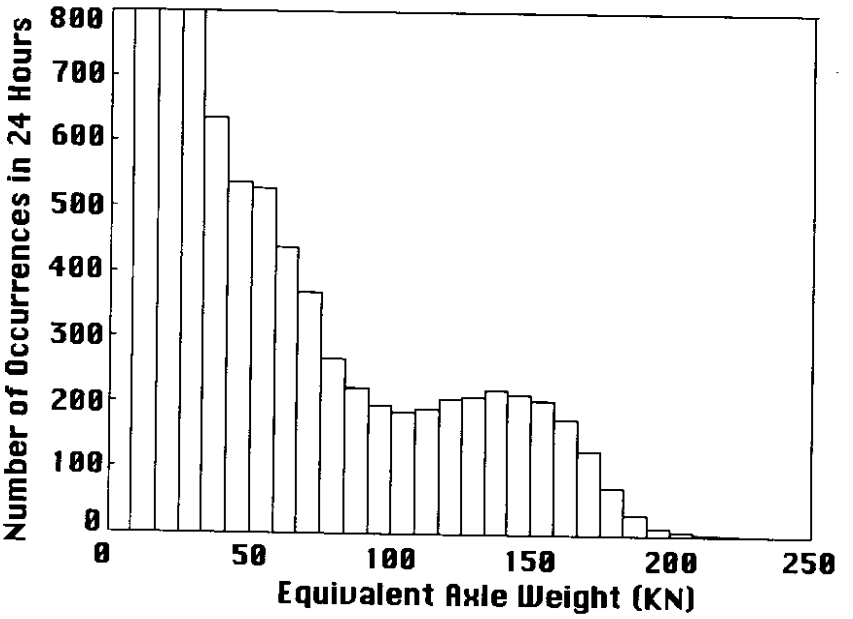

Figure 38. Estimated Truck Axle Load Spectrum for Toutle River Bridge

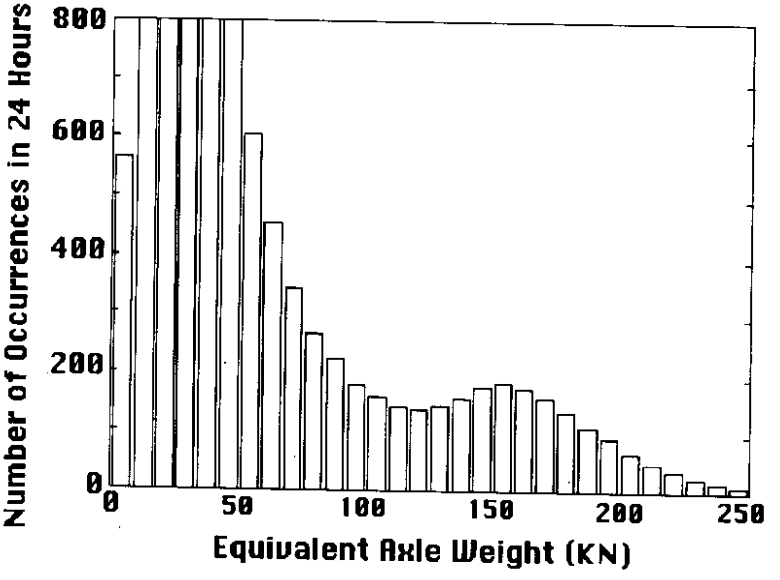

Figure 39. Estimated Truck Axle Load Spectrum for Lewis River Bridge

heaviest daily truck traffic was found to occur on the weekdays, Monday through Friday. Saturdays appeared to have only about 40 to 50 percent of the heavy trucks typical on weekdays, and Sundays had 20 percent of weekday truck traffic. Variations during the day were also noted, but the largest number of trucks were noted during the daylight hours, and the relatively largest number of heavy trucks were noted in morning hours after daylight.

WSDOT historic traffic data were used to examine month to month and year to year variation because it had a significant impact on fatigue life evaluation. For this adjustment, the average daily traffic volume for each bridge was estimated from compiled traffic data (WSDOT 1950-95, WSDOT 1993). These data suggested that the August- September period is slightly below average, and so the histograms of Figures 36 through 39 were adjusted by this small percentage to achieve an estimated average for 1996. Past traffic data were then used to translate these curves to past years. Figure 40 shows the average daily traffic volume for these two bridges over past years.

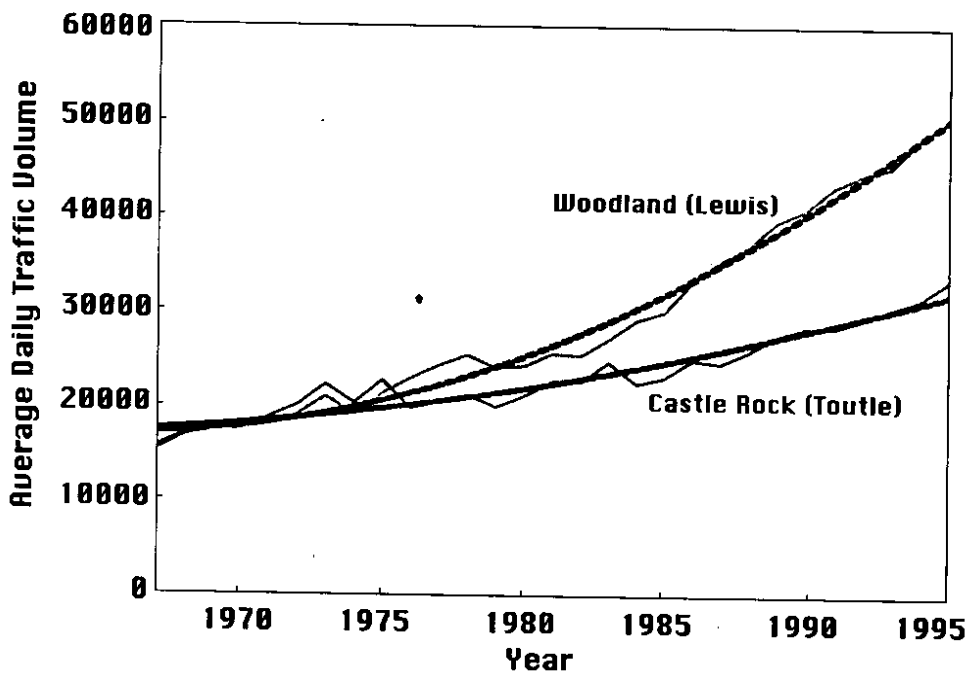

Figure 40. Average Daily Traffic For Both Bridges

The total daily traffic volume was adjusted to a total daily truck traffic volume by the average truck count data included in the WSDOT statistics (WSDOT 1950-1995, WSDOT 1993). However, for the actual calculations, a curve fit to the actual data was employed. The figure shows two curves for each bridge site. The irregular curve is the actual estimated data for the years, and the smooth curve is the curve fit to these data. Then the mix of truck weights obtained in the 1996 field measurements was applied to the truck volume postulated for these earlier years (as well as for future years).

The data of Figure 40 raise a serious question that has considerable impact on the fatigue evaluation. The traffic data suggest that the Lewis River bridge has carried a considerably larger volume of traffic than the Toutle River bridge. This must be a question of some concern, since both bridges are on the southbound lanes of I-5 and are located less than 50 km apart. Kelso and several other small towns lie between the two bridges, but the combined population of these towns is approximately 30,000 people. This population is rather small to explain the 20,000 vehicles (or 3,500 trucks) per day difference predicted for 1995 for the two bridge sites. Kelso-Longview is a seaport, and there is also an alternative route to the Oregon coast that intersects I-5 between these bridges. Nevertheless, the difference in volume seems large. This large difference in volume had a significant impact on the fatigue predictions.

The future truck traffic volume predictions were largely dependent upon a recent WSDOT study on truck traffic volumes for the region (WSDOT 1993), but this study did not provide specific data for the two bridge sites. As a result of WSDOT traffic estimates for past years, the difference in predicted truck traffic volume grows relatively larger in future years. The consequence of this difference is a significantly longer predicted fatigue life for the Toutle River location than for the Lewis River site. It is unclear whether this big difference is truly rational, and so the fatigue lives predicted for the Toutle River site could be viewed as upper bound estimates.

FATIGUE LIFE ESTIMATES

The measurements described earlier can readily be translated into stress histograms through rain flow analysis (Wirsching and Shehata 1977). The truck volume histories and correction factors described in the previous section can then be applied to the measured stress histograms to obtain stress histories over many years of service. The S-N curves relevant to a given detail, as described in Chapter 2, can then be combined with this lifetime stress history in the Miner's rule accumulated damage model (Equation 1) to estimate the fatigue life of critical elements of the bridge structure. Note that the slope of S-N curves is normally minus 1/3 in the log-log format. This means that

$$\log S_r = \log S_1 - \frac{1}{3} \log N_i \qquad \text{(Equation 4)}$$

or

$$N_i = \frac{S_1^3}{S_r^3} \qquad \text{(Equation 5)}$$

where S_r is the allowable stress range as a function of the number of cycles, N_i, for the stress range category. The value S_1 represents the stress value at the intercept of the S-N curve at 1 cycle, and this value distinguishes the different fatigue categories from each other. Note that S_1 is the cube root of the variable A, which is used in the fatigue provisions of the AASHTO LRFD Specifications. Under these conditions the fatigue life ratio can be estimated from the stress histogram. That is,

$$\text{Fatigue Life Ratio} = \sum \frac{n_i}{N_i} = \sum \frac{n_i S_r^3}{S_1^3} \qquad \text{(Equation 6)}$$

When the ratio is less than 1.0, the component has not yet reached its fatigue life. When the ratio exceeds 1.0, fatigue failure can be expected. These estimates were completed for critical elements on both bridges.

Stringer Cope at Stringer to Floorbeam Connection

Much of the fatigue cracking noted on WSDOT riveted steel bridges occurs at the coped connections between the stringers and floorbeams, and these connections were analyzed for both bridges. The analysis of these connections required consideration of the end rotational restraint, discussed in an earlier chapter. Previous research (Yam and Cheng, 1990) showed that fatigue of these connections is sensitive to the moment at the critical cope, which depends upon end restraint. Previous research also noted that Category C is a lower bound estimate for initial visible cracking in the connection. Category B is estimated to be a better indication of the fatigue life. Figures 41 and 42 show the fatigue life ratios as a function of time for the Toutle River and Lewis River bridges, respectively.

Figure 41 suggests that the Toutle River bridge will have used less than 70 percent of its fatigue life by the year 2020 AD. This suggests that fatigue cracking at this location is not a serious problem for the Toutle River bridge. Note that no cracks have been observed at this connection at the Toutle River site. Figure 42 suggests that cracking should be noted at these connections for the Lewis River bridge starting in the mid-1980s and full fracture of these connections should be expected by approximately 2005 AD. In evaluating these observations, it must be recognized that the AASHTO S-N curves are selected to be approximately 2 standard deviations from the mean. Thus, fracture would be expected only on a small portion of these elements at the times noted. Furthermore, the stress range will have achieved the largest number of cycles only for the stringers under the right hand lane. This again appears to be consistent with observed behavior on the Lewis River bridge, since a number of cracks have been noted primarily in the stringers under the right lane. The S-N curves used in this analysis were the S-N curves for non-redundant stress conditions. Non-redundant S-N curves have an allowable stress range that is 80 percent of that for the normal redundant curves. When this decrease in the stress range is

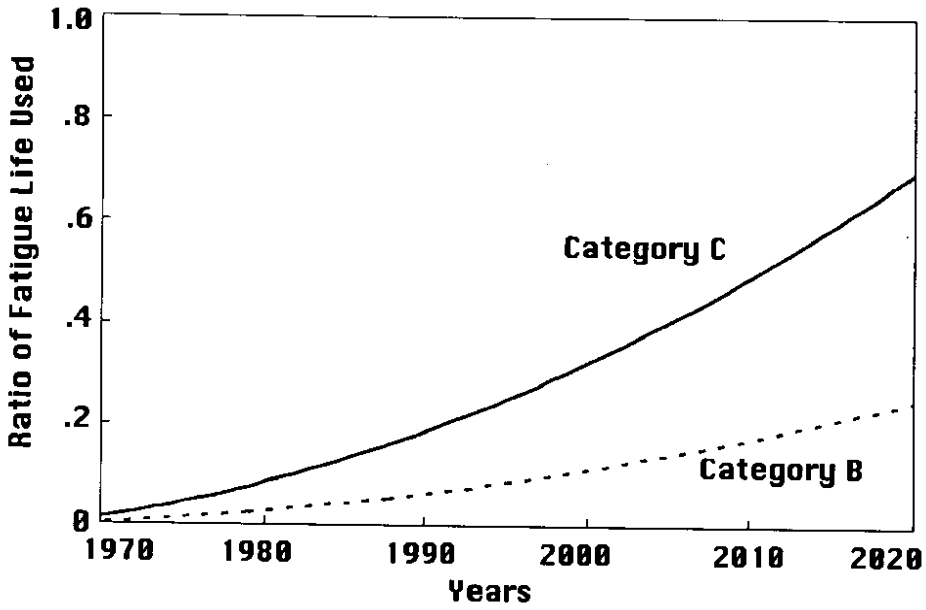

Figure 41. Estimated Fatigue Life for Stringer Cope Detail on the Toutle River Bridge

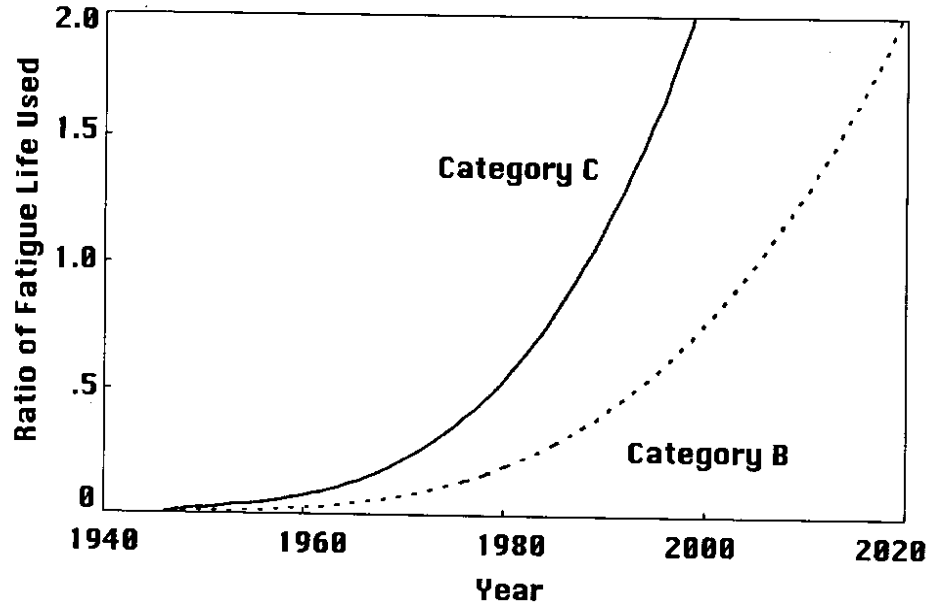

Figure 42. Estimated Fatigue Life for Stringer Cope Detail on the Lewis River Bridge

applied in Equation 4, the fatigue life ratio is reduced to approximately 51 percent of that expected with redundant S-N curves. The issue of redundancy is important because the stringers are closely spaced in parallel, and some load sharing clearly occurs. The net effect of these factors is that the curves in Figure 42 and 43 must be treated as lower bound estimates of the true fatigue life. The use of redundant fatigue S-N curves would mean that fatigue fracture should not occur until a fatigue life ratio of nearly 2.0 has been achieved. However, the good agreement between these Lewis River predictions and the actual cracking noted on that bridge suggest that this lower bound is not too far from the true solution.

The large difference in the fatigue life expected for the stringers for the Lewis River and Toutle River bridge was somewhat unexpected because the Toutle River bridge stringers are smaller, with larger spacing, than the Lewis River bridge stringers. The primary factors that contribute to this reduced fatigue life are the greater number of truck cycles and the greater end restraint measured for the Lewis River Bridge stringers. One may question whether the end restraint is maintained after cracking occurs. Ductile behavior would reduce this end restraint, and this ductility could extend the fatigue life of the elements, but fracture is not a particularly ductile mode of behavior. Furthermore, the previous discussion showed that Figures 41 and 42 are lower bound estimates of the fatigue life. As a result, the fatigue life calculation was modified to evaluate the maximum fatigue life that could be expected under the most favorable circumstances. This modified calculation is a clear upper bound and can be achieved only if significant ductility is retained in the cracked connection. It assumes no rotational restraint at the stringer-to-floorbeam connection and employs redundant S-N curves. Figure 43 illustrates this upper bound estimate for the Lewis River bridge. This figure shows that if this ductility is achieved, fatigue fracture is a far less serious problem at this location. This figure also shows that elimination of the end rotational restraint of the stringer-to-floorbeam connections could

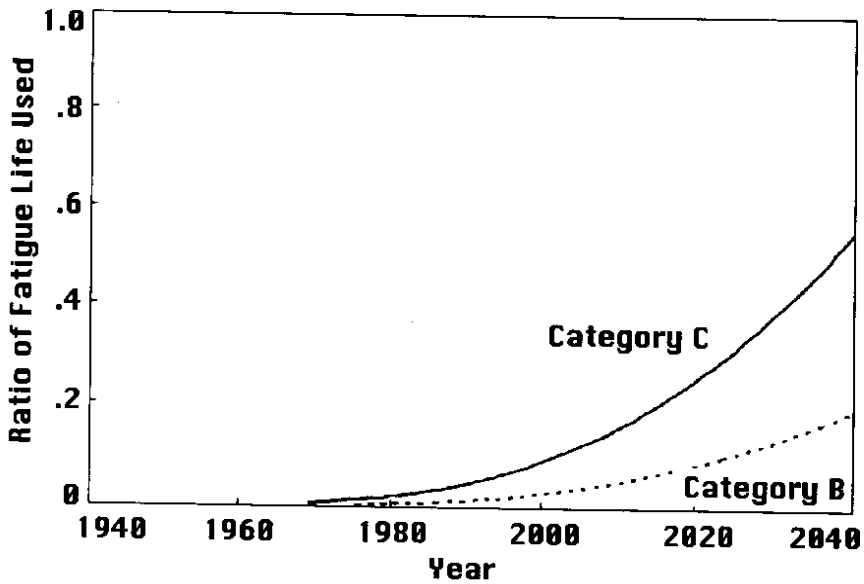

Figure 43. Maximum Upper Bound Fatigue Life Estimate for the Stringers on the Lewis River Bridge

significantly increase the fatigue life of these connections. These analyses provide no information regarding the repairs made to these connections, and this remains a question of further consideration.

The stringers and stringer connections of both bridges were evaluated at other locations away from the coped joint. There is little potential for fatigue cracking of the stringer members at either bridge site. The connecting angle between the stringer and floorbeam has a medium potential for failure at both bridges.

Floorbeams and Floorbeam-to-Chord Connections

The floorbeams and the connections between the floorbeams and the tie chord of the arch or hangers of the truss were also evaluated. The floorbeams and floorbeam-to-hanger connections of the Lewis River bridge are somewhat more susceptible to fatigue fracture than the comparable elements of the Toutle River bridge. In general, the floorbeam and its connection for the Toutle River bridge will have used only 30 to 40 percent of its fatigue life by 2040 AD. The connection between the floor beam and the chord on the Toutle River

bridge is more susceptible to fatigue than the member itself. It is the part of the floorbeam that may need more frequent inspection because significant rotational end restraint is developed in these connections. Because of limited fatigue potential for the Toutle River bridge, no further discussion of these elements is provided.

The floorbeams and floorbeam connections of the Lewis River bridge required additional consideration. The connection between the floorbeam and the truss hangers develops very little rotational restraint, and so the connection appears to be less susceptible to fatigue than the floorbeam member. The floorbeams for the Lewis River bridge are riveted, built-up members with multiple riveted coverplate terminations, as illustrated in the sketch of Figure 44. There is limited information for selecting S-N curves for elements of this type, but research by Fisher suggests that the elements may initiate visible cracking when the stress range history reaches the Category D S-N curve, and fatigue fracture may conservatively be estimated with Category C S-N curve. There is no redundancy for these floorbeams, so the more conservative non-redundant S-N curves were employed. The members were checked at maximum moment and other critical locations. Ultimately the second cover plate termination was found to be the most critical location, and Figure 45 shows the fatigue life predictions for this coverplate termination. This critical termination point is well within its fatigue life, but cracking may be expected in the coming years. Because Category C is probably a conservative estimate of fatigue life, the figure suggests that cracking at these locations can be anticipated during the years 2005 to 2025 AD. Beyond this critical location, it appears that the floorbeams of both bridges are less sensitive to fatigue cracking than other parts of the structure.

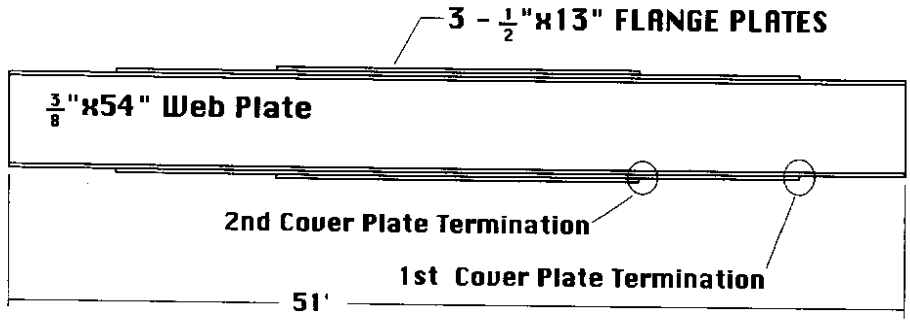

Figure 44. Sketch of Typical Built-up Floorbeams on Lewis River Bridge

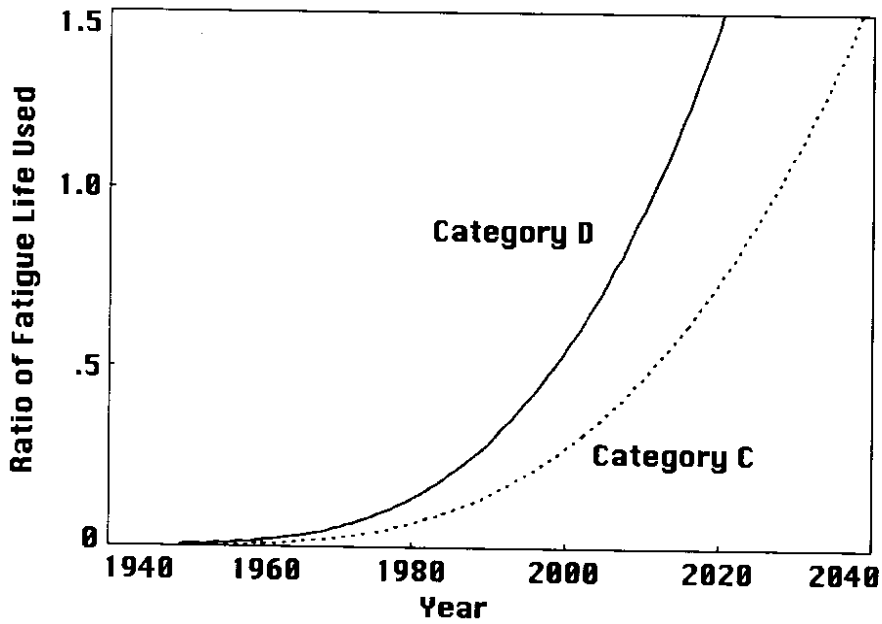

Figure 45. Estimated Fatigue Life of the Floorbeam at the Second Coverplate Termination.

It is surprising that the floorbeams of the Lewis River bridge are more sensitive to fatigue cracking than the floorbeams of the Toutle River bridge, since numerous cracks have been noted on the Toutle River floorbeams but none have been noted for the Lewis River floorbeams. Later discussion will elaborate on this issue and show the causes of this apparent discrepancy.

Fatigue of Truss Members

Fatigue of the truss members of the Lewis River bridge is of particular interest. It is of interest because the truss members have no redundancy and are essential to the safety and serviceability of the bridge. Furthermore, a recent fracture of a truss chord described in Chapter 1 raises concerns about these members' sensitivity to fatigue cracking. The instrumented truss members were evaluated. Categories C and D were used for the riveted members and connections, and the non-redundant S-N curves were employed. The instrumented members were checked directly, and other truss members were checked by combining the results of the computer analyses described earlier with the field measurements noted here. None of the truss members were found to be near their fatigue lives. Figure 46 shows the fatigue life estimates for one of most critical members in the Lewis River bridge truss, and it can be seen that the member will have achieved only 20 to 40 percent of its fatigue life by 2040 AD.

The analysis indicates that fatigue should not be regarded as a problem for the truss members and connections of the Lewis River bridge for many years to come. However Figure 4 clearly shows that one such fracture has already occurred on another bridge in Washington State. This raises the question of whether the Lewis River bridge has dramatically different stress levels than other riveted truss bridges in the state. This research study did not check the stress levels on these other bridges. However, it appears unlikely that the stresses would be dramatically different because the bridges were designed by the same engineers at similar times with similar materials and technology. Therefore, some consideration was given to why cracking has occurred on one bridge while calculations indicate that it is unlikely to occur. This analysis isolated a potential concern regarding the fatigue life of these truss members.

The assumption made in design, analysis and these field measurements is that the stresses in truss members are uniformly distributed over the member. This need not be the

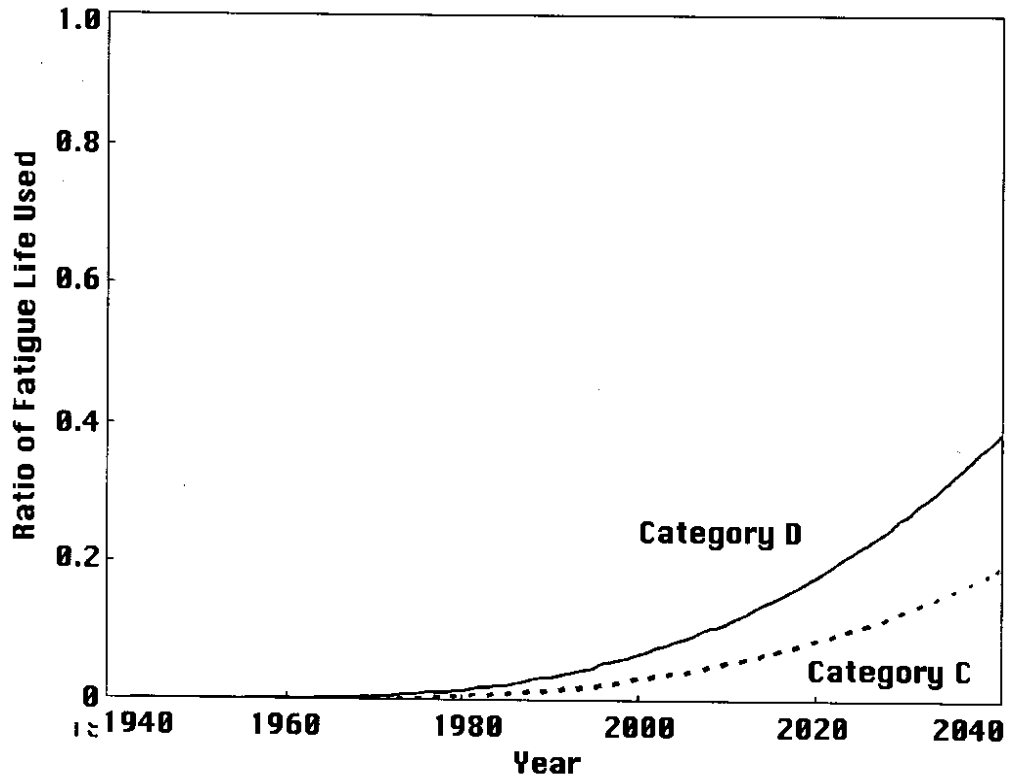

Figure 46. Fatigue Life Predictions for the Most Severe Connection in the Bridge Truss of the Lewis River Bridge

case. Stress is unlikely to be uniform if the rivets are loose or deteriorated. Non-uniform stress may be caused by irregularities in the fabrication, local yielding, impact damage, or buckling of elements in the built-up section. The effect of a non-uniform stress on the fatigue life could be dramatic. In an extreme case, all of the force could be carried by one element of the built-up section, and the average stress in the loaded element would be at least two times the average for the total section. This local stress distribution would increase the stress range in the loaded element by a similar ratio. If the stress range is doubled, Equation 8 shows that the fatigue life is reduced to 0.125 of that expected with a uniform stress distribution. Figure 46 shows that the curves could achieve a ratio of 0.125 at any time, so the possibility of this non-uniform loading should always be an issue of concern in inspection and evaluation of these riveted truss members.

Chord and Arch Members

The fatigue life and potential for fatigue cracking of the chord and arch members of the Toutle River bridge were also examined. This evaluation also required extensive use of the results of computer analysis because there are a number of potential crack locations. These locations include splices and joints, weld locations for stiffeners and tie plates, and the location of maximum moment in the arch and chord elements. In general, the chord and arch are not particularly sensitive to fatigue, since fatigue cracking was not predicted until 2040 or later. However, the bottom flange tie plates are welded to the bottom flange of the chord. This constitutes a Category C detail, and it occurs at some locations that are highly stressed by truck loading. The fatigue evaluation of this detail appears to be most critical for the Toutle River bridge structural system, and its fatigue life estimate from non-redundant S-N curves is shown in Figure 47. This curve shows that fatigue fracture of these locations may be expected after 2015 AD.

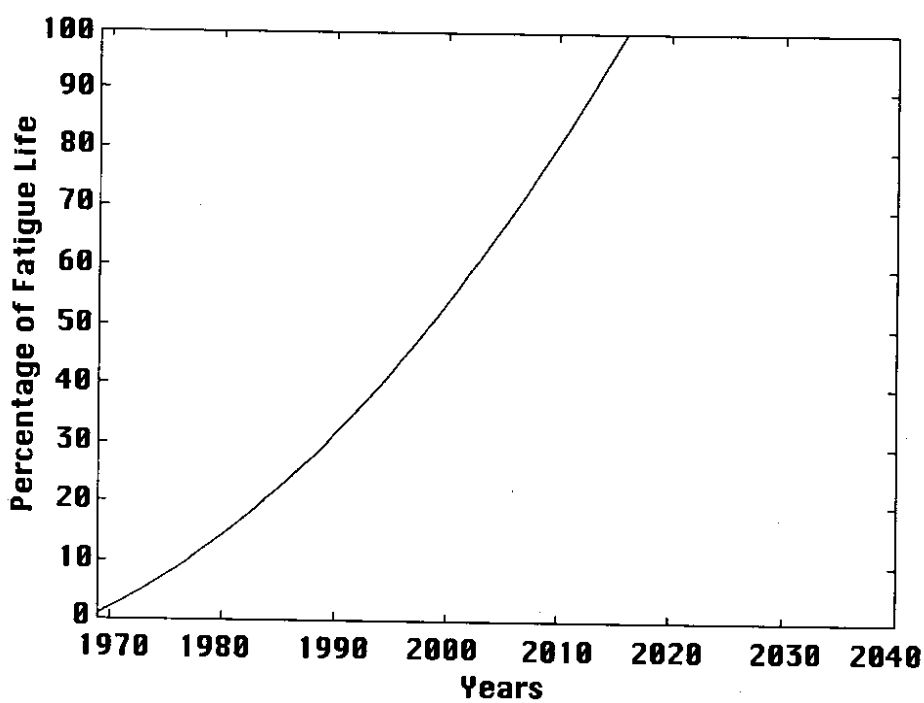

Figure 47. Fatigue Life Prediction for Tie Chord of the Toutle River Bridge

DISTORTIONAL FATIGUE

Extensive cracking has been noted in the floorbeams of the Toutle River bridge, but the fatigue stress calculations suggest that these floorbeams are not the most fatigue sensitive portions of the structure. Previous discussion of the analysis and controlled test results noted that the Toutle River bridge is particularly prone to large deflections, vibrations, and local deformations. In particular, significant twisting of the floorbeams relative to the stringer and chord rotation was measured. Evaluation of this deformation indicated that fatigue cracking of the floorbeams of the Toutle River bridge is driven by distortional based fatigue. The distortion induces tensile stresses in the members, but the tensile stresses are not easily nor uniquely computed because they are the stresses caused by local deformation and distortion.

The evidence of distortional fatigue is very strong. It is provided by the measured response in the controlled truck testing and the sequence of cracking noted on the Toutle River, combined with the measured and computed response at various stages of the bridge history.

The measured response of the bridge showed that the chord deflects approximately as a full sine wave when a truck crosses the Toutle River bridge. This sine wave deflection is a manifestation of the first mode of vibration. It is excited by the movement of the truck across the bridge, as illustrated in Figure 48.

These large deflections cause time dependent rotations of the chord and the end of the floorbeam because the ends of the floorbeams are attached to the chord. The bridge deck lies on the top flanges of the stringers and floor beams, which are at the same level as the top of the chord. Figure 48a shows that the deflected shape of the bridge induces tensile stress in the right hand portion of the bridge deck and compressive stress in the other half of the deck slab. Figure 48b shows that these stresses are reversed when the truck moves to the 3/4 span portion of the bridge deck. Although the deflected shape attempts to axially deform the deck, it is unable to do this effectively. The floorbeams are

not stiff enough or strong enough in torsion or weak axis bending to develop these forces and moments needed to deform the deck. As a result, significant twisting of the floorbeam occurs over the short length between the tie chord and the first one or two stringers.

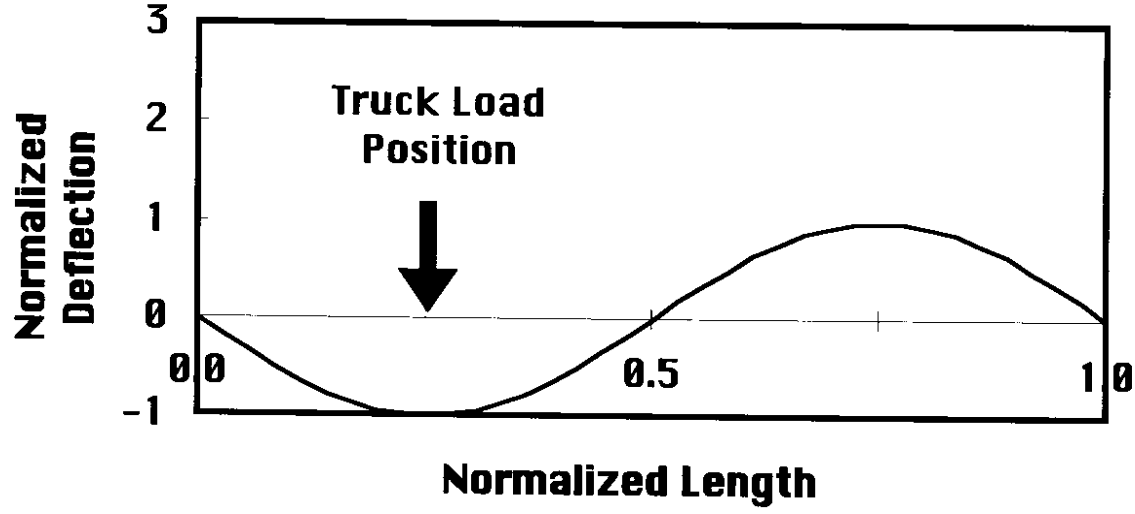

a) Truck at Quarter Point

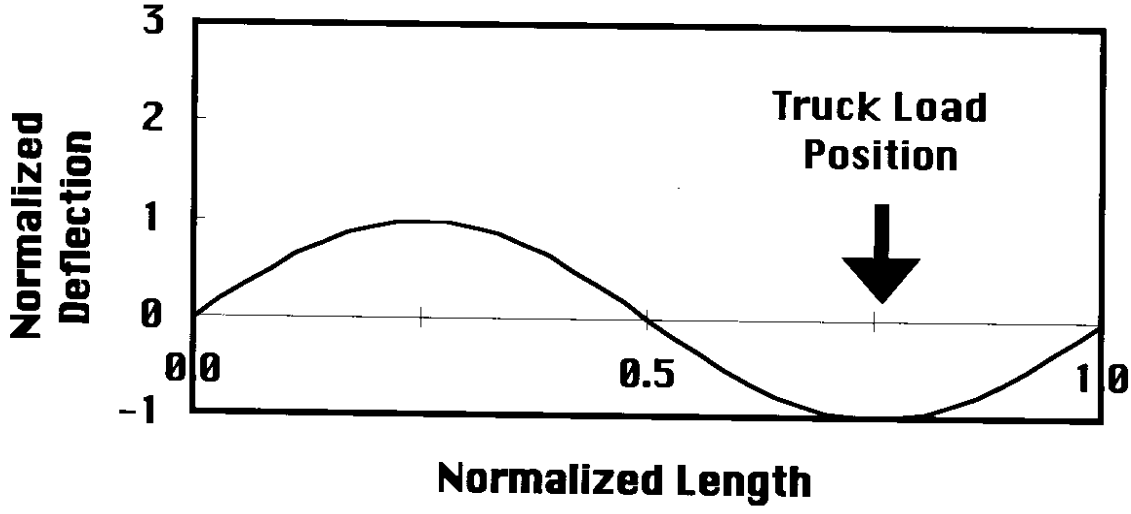

b) Truck at the Three Quarter Point

Figure 48. Deflected Shape of Chord of Toutle River Bridge with Relationship to Truck Position

Some shortening or lengthening of the top of the chord occurs because of limited compressive or tensile stress developing in the slab, as noted earlier. However, there must be relative movement between the deck and the top of the chord because the floorbeams are unable to transmit the large forces and moments necessary to fully stress the slab. This twisting and differential rotation was measured (Crocker 1997) in the experiments. At the same time, relative movement between the deck slab and the steel framing was measured. This differential slip and differential rotation and twist are the main contributing factors to the deformation driven fatigue in the Toutle River floorbeams.

This distortional fatigue can also be verified by examining the crack history of the Toutle River Bridge. Before 1989, the top flanges of the interior floor beams were not connected to the chord, and so the differential deformation was concentrated in the web between the web angles and top flange, as illustrated in Figure 49. This led to web cracking at all of these locations. After 1989, the top flanges of the floorbeams were attached to the top flange of the chord. This attachment prevented the local deformation of the web at the ends of the floor beam, as shown in Figure 49. Never the less, the differential rotation is still present, and the modified connection has made the floor beam only slightly stiffer in torsion and weak axis bending. As a result, the bulk of the deformation moved to another location. This alternative location is the web of the floorbeam at the stringer-to-floorbeam connection. This local deformation has led to high tensile stresses in this local region, and cracks in the floorbeam webs near the first interior stringers have been seen since 1989.

The deformation noted above results in a large differential movement between the abutment floorbeams and the deck slab. Before 1989, the top flange of the abutment girders was attached to the top flange of the chord through a riveted flange plate. The slip deformation induced weak axis bending of the floorbeams and the flange plate, and the flange connection plate constituted a Category B fatigue detail. Unfortunately the

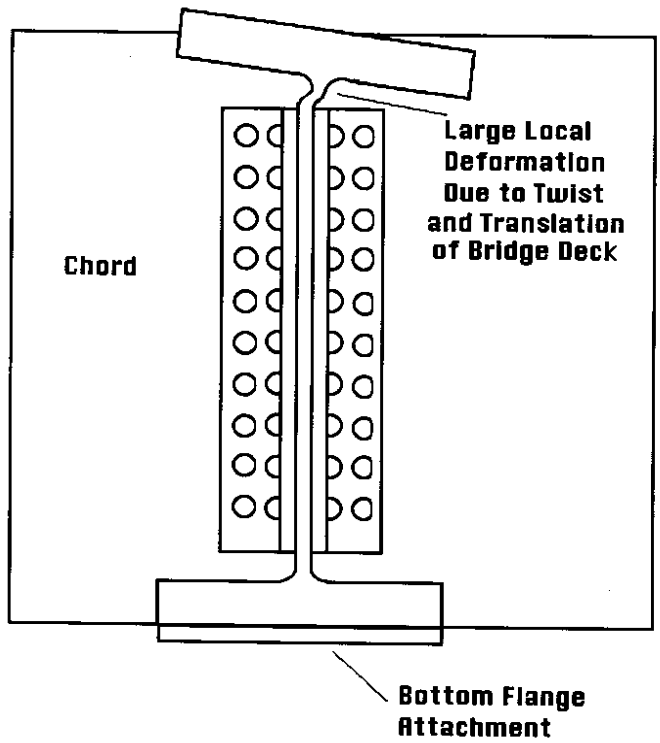

Figure 49. Local Deformation in Floorbeam Web at Floorbeam to Chord Connection

magnitude of the moment is not determinate, but this moment induced fatigue cracking through the tie, which was observed in the early years of the bridge. These cracked plates were replaced several years ago.

Because this floorbeam web cracking and the flange plate cracking are driven by deformation, it must be expected that this cracking will continue as the deformations continue. Both the floor beam web cracking and flange plate cracking will occur on both sides of the bridge. Fortunately, the past web cracking has occurred in an area that does not immediately impact the safety of the bridge, but the deformational nature of the cracking suggests that drilling holes will not be an effective repair. Reinforcement of these areas will likely drive the cracking to adjacent areas. However, the severity of the stress at the crack tip may be reduced as the crack lengthens, since much of the deformation is taken up without developing larger stresses. Therefore these cracks may eventually stabilize after they have reached an adequate length. Elimination of this cracking will otherwise require

elimination of the local deformation. The Toutle River bridge is particularly lively in its response to truck loading, and substantial measures would be needed to eliminate this deformation. Possible revisions are discussed in the next chapter.

SUMMARY, CONCLUSIONS AND RECOMMENDATIONS

SUMMARY

The Lewis River and Toutle River bridges have experienced significant cracking due to fatigue loading. These bridges are typical of riveted truss and tied arch bridges throughout the state. The cracking on these two bridges was reviewed and analyzed. Computer models of the two bridges were developed, and static and dynamic analyses were performed. The results of the analyses were combined with the observed damage patterns to develop an instrumentation plan for the two bridges. Strain gages and potentiometers were installed on both bridges, and accelerometers were installed to infer global deflections of the Toutle River bridge. Controlled load tests were performed on the two bridges in August 1996 with trucks of known weight and geometry traveling at known speeds in the various driving lanes of the two bridges. The results of these measurements were used to evaluate the overall behavior of the two bridges and to calibrate the strains and deformations for further testing with trucks of unknown weight and geometry. A limited series of weigh station tests supplemented these calibration data.

Upon completion of the calibration tests, uncontrolled truck traffic was measured for the two bridges for nearly one month. These measurements were used to generate load spectrum data for the two bridges. These statistical data were combined with historic truck traffic data and predictions for future traffic to estimate fatigue life for critical components of both bridges.

CONCLUSIONS

A number of conclusions were drawn from this research. These include the following.

1. The Toutle River Bridge is a steel tied-arch bridge that has experienced significant cracking in the floorbeams and floorbeam-to-tie

chord connections. The bridge is quite flexible and is very susceptible to large deflections and vibrations as a result of truck loading. Although the deflections and vibrations are large, there is little or no amplification of the dynamic response. The fundamental vibration has a period of approximately 1.11 seconds, and damping was estimated to be 0.5 percent of critical. As a result of the small damping, the dynamic response caused by heavy trucks continues for more than 10 or 20 seconds after a truck has left the bridge.

2. The Lewis River bridge is a riveted steel bridge that has sustained significant cracking in the coped stringers and stringer-to-floorbeam connection. The bridge is relatively stiff in comparison to the Toutle River bridge. The period of the first mode of vibration is approximately 0.48 seconds, and there is little or no amplification of the dynamic response.

3. The floorbeams of both bridges do not have shear connectors between the slab and floorbeam. Limited composite action was noted for both bridges, but it is so small that it does not have great effect on the floorbeam behavior.

4. The connections between the truss hangers and the floorbeams of the Lewis River bridge are partially restrained, but the rotational restraint of this connection has little impact on the floorbeam behavior because the restraint for the interior floorbeams is limited by the flexibility of the vertical hanger and chord. The connection between the floorbeams and the chord of the Toutle River bridge are stiffer, but the rotational restraint here is limited by the torsional stiffness of the chord. This end restraint is larger than that noted on the interior floorbeams of the Lewis River bridge, but it still does not significantly change the moment diagrams for the floorbeams.

5. The stringers of the Lewis River bridge have no shear connectors whereas the Toutle River bridge had shear connectors over the length of the stringers. Despite this difference, the composite actions in the stringers of the Lewis River bridge are as large or larger than those seen for the Toutle River bridge. The composite action is 40 to 60 percent of fully composite for stringers directly under the right hand lane of the Lewis River bridge and between 40 and 50 percent of fully composite for the stringers under the right hand lane of the Toutle River bridge. The composite action is typically larger for lighter loads and lightly loaded members. Therefore, larger composite action (80 to 100 percent) was noted for stringers under the shoulder or for stringers with trucks in adjacent lanes.

6. The connections between the stringer and floorbeams are variations of coped web angle and coped seated beam connections in both the Lewis River and Toutle River bridges. These connections provide significant rotational end restraint to the stringers of both bridges. Although the magnitude of the end restraint is comparable for both bridges, the end restraint has a large effect on fatigue life estimates for the stringers on the Lewis River bridge and relatively little effect on the Toutle River bridge stringers.

7. The uncontrolled truck measurements were combined with calibration factors established through the controlled testing and weigh station testing to develop load spectra for both bridges. The spectra are approximate because the calibration is approximate, and they do not account for the variations in truck geometry or cases in which more than one truck is on the bridge at a given time. The comparisons of the spectra were good, indicating that the data are valid and comparable for both bridges. Modest

variations were noted, but these are consistent with the approximations noted above.

8. Historical traffic data were examined for both bridges, and they were combined with the statistical accumulation of the uncontrolled truck measurements to produce fatigue estimates for both bridges. The best available WSDOT truck traffic data were used, but there are dramatic differences in the projections for the two bridges. A much larger volume of truck traffic is predicted for the Lewis River bridge than for the Toutle River bridge. The magnitude of this difference is so much larger that it strains the intuition of the research team. The difference also has a significant effect on the fatigue life predictions. If it is agreed that the difference is too large, the consequence would be that the projected fatigue life of the Toutle River bridge could be too long or the projected life of the Lewis River bridge could be too short.

9. There is further uncertainty in the fatigue life predictions in that experimental information regarding the fatigue life of riveted members and connections is very limited. As a result, there was ambiguity in the selection of the S-N curves for the analysis. Upper and lower bound estimates were made to address this uncertainty. The limits summarized in these conclusions emphasize the estimates in which the authors place greater confidence.

10. The present fatigue cracking in the Lewis River bridge is at the copes of the stringers. Given the measured truck traffic and the projected traffic growth rates, the lower bound estimates indicate that cracking should already be expected. A number of cracks have been observed in recent years, so this lower bound estimate appears rational. These same indicators suggests that fracture of these coped stringer joints is possible starting

somewhere between 2005 and 2010 AD. The statistical nature of the S-N curves and the variations in loading on different stringers mean that fracture is most probable under the more heavily traveled right hand lane, and analysis suggests that no more than 5 percent of those stringers would be at the threshold by the projected date of 2005 AD.

11. The floorbeam-to-hanger connections of the Lewis River bridge are not expected to sustain cracking for many years because of the small rotational restraint at that location. However, the terminations of the riveted coverplates are candidates for fatigue cracking. In particular, cracking may start near the second coverplate termination of interior floorbeams between 2005 and 2015 AD. Fatigue fracture at this location does not appear likely until approximately 2025 AD.

12. The truss members of the Lewis River bridge are not susceptible to fatigue cracking for at least 50 years. Although the probability of this cracking is slight, the consequences would be severe. Therefore, plausible reasons for cracking in the chord or truss members earlier than predicted were examined. The chord members are built-up sections, and the distribution of forces in the built-up members may not be uniform. Note that the instrumentation used in these field measurements was not set up to establish the uniformity or non-uniformity of member loading because the cost of such testing would have been nearly doubled. Non-uniformity may be caused by impact damage, looseness of rivets, or excess distortion induced during fabrication and erection. Extreme non-uniformity in load distribution has a dramatic effect on fatigue life. If extreme distributions exist, it is possible that fatigue fractures could occur before 1997 AD.

13. Fatigue cracking of the floorbeams of the Toutle River bridge is dominated by distortional fatigue. It is caused by the large dynamic deflections and deformations noted in the bridge. Stress induced fatigue should not be a problem in these elements for a number of years. Distortional-based fatigue is no less serious nor no more serious than stress induced fatigue, but methods for predicting fatigue life do not exist. Therefore, the fatigue life is not easily calculated. It is possible that the cracks will stabilize after having reached an adequate size. Fisher (1984) has suggested that the hole drilling method can be effective in controlling the crack growth with distortional fatigue. However, with the distortions measured on the Toutle River bridge, the researchers are confident that the hole drilling method will not be effective until the cracks are at or very near a stable length. Distortional effects will likely cause further cracking at other locations of the floorbeam, but it is impossible to predict the fatigue life of these elements with present knowledge.

14. The arch and chord of the Toutle River bridge are not likely to be affected by the distortional fatigue and it does not appear that they will be sensitive to stress induced fatigue cracking until approximately 2040. However, critical locations of the chord with maximum bending moment sometimes have a welded plate attachment. The maximum moments are normally near the quarter points of the bridge span. Fatigue cracking at these locations is possible by approximately 2015.

DISCUSSION OF RECOMMENDATIONS

The above conclusions provide some predictions of fatigue life for critical elements of the Lewis River and Toutle River bridges. The predictions were made with the goal that the logic and reasoning could be applied to other similar bridges in the WSDOT inventory.

Decisions regarding future actions for these bridges are largely dominated by economic concerns and are beyond the scope of this study. However, the conclusions led to several clear recommendations regarding future inspections of these and similar bridges. These inspection recommendations are as follows.

1. The distortion induced fatigue in the tied arch bridge is a concern that cannot easily be quantified. Continued regular inspection of these locations is clearly appropriate.

2. The coped stringer locations are prime candidates for fatigue cracking on the Lewis River bridge. The hole drilling method appears to be limiting the crack growth, but there is no evidence to verify that this is in fact the case. Continued regular inspection (particularly under the most heavily traveled lanes) is also clearly appropriate.

3. The coverplate terminations on interior riveted floorbeams of the Lewis River bridge appear to be candidates for cracking in the not too distant future. Therefore, emphasis on the inspection of these locations seems appropriate.

4. The tie chords of the Toutle River bridge at the weld bottom flange attachments near the quarter or third span locations appear to be candidates for cracking in the not too distant future. Therefore, emphasis on the inspection of these locations is also appropriate.

5. The flange tie plates on the Toutle River bridge are likely candidates for further distortion induced cracking. However, these elements are not directly needed for safety and serviceability of the bridge, so inspection is somewhat less critical on these elements.

6. Finally, the truss members are not very sensitive to fatigue fracture, but they become very sensitive to fatigue cracking if the stress is not uniformly distributed in the member. It is recommended that during

future truss inspections inspectors be watchful for conditions that lead to non-uniform loading.

As noted earlier, rational decisions regarding the future of these bridges require economic data and other information that is beyond the scope of this study. However, several ideas for possibly extending the fatigue life of these and similar bridges are worthy of some discussion.

1. The fatigue cracking in the Toutle River bridge is driven by distortional fatigue induced by the large bridge deformations. A primary method for eliminating this fatigue is to eliminate the distortional deformation. One plausible method is to attach diagonal cables, as depicted in Figure 50. This should dramatically stiffen the bridge, reduce the deflections and deformations, and as a consequence eliminate the deformational fatigue. There would be some major difficulties. All of the hangers and diagonals are cables and so they must remain in tension. Therefore, the design of a scheme of this type would need to assure that the cables could be pretensioned to avoid slack cables or compression in the hangers. However, if this can be achieved, the increased stiffness could well eliminate all fatigue problems with these bridges for many years to come.

Note that similar damage was found on another steel tied-arch bridge (Mertz 1998) in Paducah, Kentucky. The cable truss option illustrated in Figure 50 was considered for repairing this bridge, but this method was not used because of concerns noted earlier. Instead, the chord of this bridge was stiffened with a stiffening truss to eliminate the problem. This stiffening truss is an alternative method for consideration.

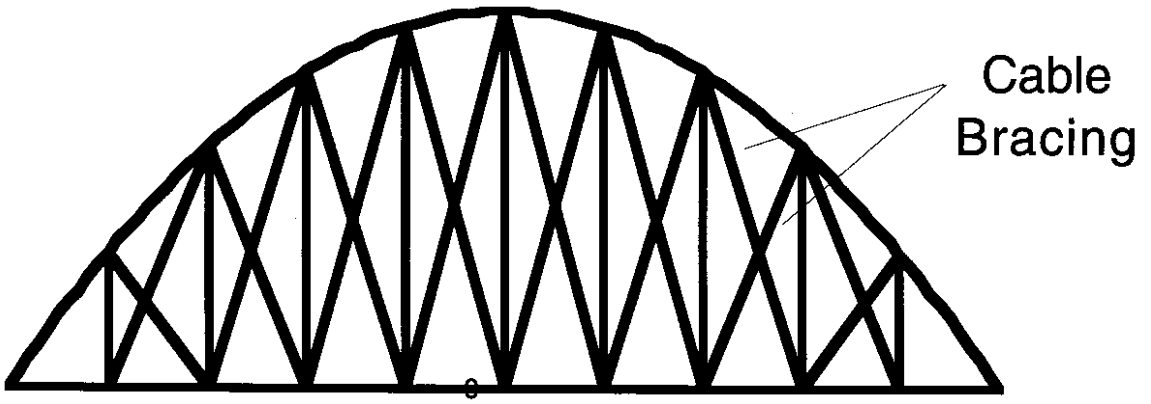

Figure 50. Possible Stiffening Method for Tied Arch Bridge

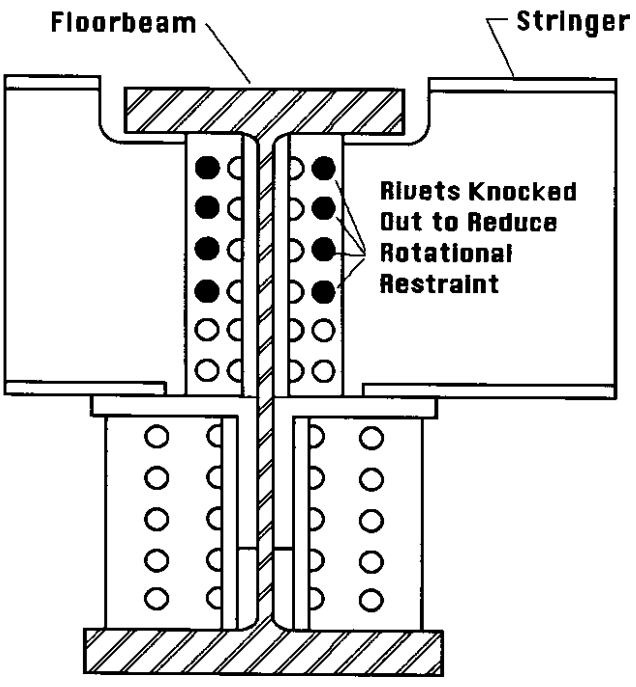

Figure 51. Possible Modification at Stringer
to Floorbeam Connection

2. A second alternative for eliminating the fatigue concerns related to the tied arch bridge hinges on the possibility of deck replacement. If the deck is to be replaced, a possible repair could be achieved by adding shear connectors to all floor beams and stringers (and possibly to the top flange of the chord). Deck reinforcement could be used to lock up the deformation of the deck. This should lock up the relative movements and stiffen the entire structure. Again, there are potential concerns. For example, this would introduce negative moments at the stringer connections, and this effect on fatigue must be considered.

3. The effectiveness of repairs such the drilled holes, fish plates and such on riveted members is not known. Experimental evidence regarding the effectiveness of these repairs or improvements to these repairs could dramatically increase fatigue life estimates with no significant modification to the bridges. Reemsnyder has tested bolts added to rivet holes, but these results do not appear to be directly applicable to this connection geometry.

4. The fatigue cracking at the copes of the stringers at the stringer-to-floorbeam connection of the Lewis River bridge is driven by the end restraint developed at these connections. Elimination of this restraint should also dramatically increase the copes' fatigue life. This could be done by knocking out some of the top rivets and adding a stiffened seat, as depicted in Figure 51. This should easily provide adequate shear resistance of the connection. This modification could possibly be concentrated under the right lane of traffic, since most of this fatigue cracking is expected there. This modification would probably result in increased connection rotation, and this could potentially result in more rapid deterioration of the deck. Therefore, the consequences of these factors must be considered.

Removel of rivets has been attempted in other states (Mertz 1998) as a method for preventing further fatigue damage on bridges. The method has sometimes been successful but in other cases it has not. Any future research must consider the flexibility conditions needed to assure the success of this method.

5. If the deck of a truss bridge is to be replaced, the addition of shear connectors to the floorbeams and stringers might have benefits similar to those noted in item 2 for the tied arch bridges.

This list of possible revisions is not exhaustive. Experienced bridge designers may clearly have many far superior suggestions for methods of improving the fatigue performance. The above concepts are submitted for purposes of discussion and consideration of the issues involved.

REFERENCES

AASHTO, "Standard Specification For Highway Bridges," American Association of State Highway and Transportation Officials, 10th Edition, Washington, D.C., 1973.

AASHTO, "Standard Specification For Highway Bridges," American Association of State Highway and Transportation Officials, 15th Edition, Washington, D.C., 1996.

AASHTO, "Guide Specifications for Fatigue Evaluation of Existing Steel Bridges," American Association of State Highway and Transportation Officials, Washington, D.C., 1990.

Arima, "Comparison of the Lewis River Bridge and the Toutle River Bridge Floor System Behavior," a thesis submitted in partial fulfillment of the Master of Science in Civil Engineering Degree, University of Washington, Seattle, WA, 1997.

Crocker, P.N., "Behavior and Fatigue of the Toutle River Bridge, a Tied-Arch Bridge on Interstate 5, Castle Rock, WA," a thesis submitted in partial fulfillment of the Master of Science in Civil Engineering Degree, University of Washington, Seattle, WA, 1997.

Fisher, John, "Fatigue and Fracture in Steel Bridges," John Wiley and Sons, New York, NY, 1984.

Fisher, J., Frank, K., Hirt, M., and McNamee, B.M, "Effect of Weldments on the fatigue Strength of Steel Beams," NCHRP Report 102. Transportation Research Board, Washington D.C., 1970.

Fisher, J., Jin, J., Wagner, D.C., and Yen, B. T., "Distortion-Induced Fatigue Cracking in Steel Bridges," NCHRP Report 336, Transportation Research Board, Washington, D.C., 1990.

Fisher, J., Yen, B.T., and Wang, D., "Fatigue and Fracture Evaluation for Rating Riveted Bridges," NCHRP Report 302, Transportation Research Board, Washington, D.C., 1987.

Frost, N.E., Marsh, K.J., and Pook, L.P., "Metal Fatigue," Oxford University Press, Ely House, London, England, 1974.

Mertz, D., personal communication to Charles Roeder on February 12, 1998.

Miner, M.A., "Cumulative Damage in Fatigue," ASME, Journal of Applied Mechanics, Vol 12, 1945.

Moses, F., Schilling, C.S., and Raju, K.S., "Fatigue Evaluation Procedures for Steel Bridges," NCHRP Report 299, Transportation Research Board, Washington, D.C., 1987.

Novak, A.S., "Calibration of LRFD Bridge Design Codes - NCHRP 12-33," University of Michigan, Ann Arbor, Michigan, 1992.

Putnam, F.A., Labtech Notebookpro, Laboratory technologies Corporation, Wilmington, MA 1996.

Reemsnyder, H.S., "Fatigue Life Extension of Riveted Connections," ASCE, Journal of Structural Division, Vol. 101, No. ST12, December 1975.

Schilling, C.S., Klippstein, K.H., Barsom, J.M, and Blake, G.T., "Fatigue of Welded Steel Bridge Memebers Under Variable Amplitude Loadings," NCHRP Report 188, Transportation Research Board, Washington, D.C., 1978.

Wilson, E.L., and Habibullah, A., "SAP90, A Series of Computer Programs for the Finite Element Analysis of Structures," Structural Analysis Users Manual, Computers and Structures, Inc., Berkeley, CA 1995.

Wirsching, P.H., and Shehata, A.M., "Fatigue Under Wide Band Random Stresses Using Rain Flow Method," ASME, Journal of Engineering Mechanics and Technology, July, 1977.

Wong, Scott, D., "Fatigue Evaluation of the I-5 Lewis River Bridge," a thesis submitted in partial fulfillment of the Master of Science in Civil Engineering Degree, University of Washington, Seattle, WA, 1997.

WSDOT, "Annual Traffic Report," Washington State Department of Transportation, Olympia, WA, 1950 through 1995.

WSDOT, "Summary of Truck Loading Patterns in Washington State," Washington State Department of Transportation, Olympia, WA, 1993.

Yam, M.C.H, and Cheng, J.J.R., "Fatigue Strength of Coped Steel Beams," ASCE, Journal of Structural Engineering, Vol. 115, No. 9, Sept. 1990.